Olsson F11

TOPOLOGICAL COINCIDENCES BETWEEN TRACKING- AND CALORIMETRIC TRIGGERS AT THE H1 EXPERIMENT

14x

Diploma Thesis of David Müller

June 1994

Completed under the supervision of Dr. U. Straumann

in the group of Prof. Dr. P. Truöl

Physik-Institut, Universität Zürich

Table of Contents 1

Abstract

For the observation of high-energy electron-proton scattering in the H1 experiment (DESY Hamburg) the first level trigger is based on two completely different systems

- The tracking triggers are derived from the information provided by the jet- and proportional chambers. One tracking trigger of special interest to this work is the so called z-vertex trigger which recognizes charged particle tracks from the interaction zone. This system is based on the data from six multiwire proportional chambers. Every combination of four cathode pads of these chambers that defines a straight line, in the following called ray, is checked. If all four pads show a signal, an entry in a histogram binned along the beam axis is made according to the origin of the ray. A trigger signal is generated, when a significant peak is found in this histogram.
- Calorimetric triggers give a positive signal when a certain amount of energy is deposited in the liquid argon (LAr) calorimeter. The calorimeter is divided into 240 solid angle sectors called big towers. The trigger electronic is built up separately for each of these big towers.

The aim of this work was to realize topological coincidences between these two systems. Big towers should be considered only when at least one ray reconstructed by the tracking triggers points in their direction. Due to this reduction of the number of big towers the system gets less susceptible to 'wrong' signals of the LAr cells caused by electronic noise or particles coming from outside the tracking system. The trigger decision should therefore become more selective.

In the first two chapters of this thesis the already existing triggers, especially z-vertex and LAr-trigger, will be explained. The third chapter shows some geometrical considerations about the combination of these two trigger systems with their limited resolution in space. The fourth chapter presents the work that was necessary to realize this new trigger: the already existing programmable electronic has been taken in use and was tested. In the last chapter the behavior of this 'big ray trigger' will be simulated on the base of 1993 data and some first runs in spring 1994. The investigations were concentrated on four classes of events: J/Psi-production due to gamma-gluon fusion, low energetic jets, charged current exchange and in contrast pure background-events.

Zusammenfassung

Bei der Untersuchung hochenergetischer Elektron-Protonstreuung am H1-Experiment (DESY Hamburg) gibt es auf der ersten Triggerstufe zwei grundlegend verschiedene Systeme:

- Ein Tracking-System, das aufgrund der Informationen aus Jet- und Proportionalkammern die Spuren der am Stoss beteiligten Teilchen zu rekonstruieren versucht, um physikalisch interessante Ereignisse möglichst schnell zu erkennen. Von Wichtigkeit für diese Arbeit ist dabei insbesondere der z-Vertex-Trigger. Dieser bildet aus den Daten von sechs Proportionalkammern alle möglichen Kombinationen von jeweils vier Kathodenfeldern ('Pads'), die eine gerade Linie ('Ray') definieren. Falls alle diese vier Pads gefeuert haben, wird ein Eintrag in einem Histogramm entlang der Strahlachse vorgenommen. Falls in diesem dann ein signifikantes Maximum auftritt, so wird einTriggersignal erzeugt.
- Verschiedene Kalorimeter-Trigger, die eine Entscheidung aufgrund der im Flüssig-Argon-System (LAr=Liquid Argon) deponierten Teilchenenergien treffen. Das Kalorimeter ist dabei in 240 sogenannte 'Big Towers' aufgeteilt, für die die Triggerelektronik jeweils getrennt aufgebaut ist.

Ziel dieser Arbeit war es nun, eine bereits vorgesehene 'topologische Verknüpfung' dieser beiden Systeme zu realisieren. Es sollen nur noch diejenigen Bereiche des Kalorimeters zur betrachteten Energiemenge gerechnet werden, auf die eine vermutete Teilchenspur des Tracking-Triggers zeigt. Durch diese Reduktion der Anzahl betrachteter Big Tower wird das System weniger anfällig auf 'zufällige' oder 'falsche' Signale, wie sie durch elektronisches Rauschen und Teilchen, die von ausserhalb des Tracking-Systems kommen, entstehen. Die Triggerentscheidung wird dadurch selektiver.

Im ersten und zweiten Kapitel dieser Arbeit sollen die bestehenden Triggersysteme, insbesondere der z-Vertex- und der LAr-Trigger in ihrer bisherigen Funktionsweise vorgestellt werden. Im dritten Teil werden dann geometrische Fragen diskutiert. Es geht dabei insbesodere darum, wie man die Verknüpfung zwischen den zwei Trigger-Systemen möglichst gut an die begrenzte Ortsauflösung derselben anpasst. Das vierte Kapitel geht auf die Anpassungen der Hardware ein, die gemacht werden mussten. Die bereits vorhandene programmierbare Elektronik wurde in Betrieb genommen und getestet. Im letzten

Kapitel wird das Verhalten des neuen Systems aufgrund von Simulationen an Daten aus der Experimentier-Periode 1993 und ersten Messungen 1994 untersucht. Dabei werden vier Kategorien von Ereignissen betrachtet: J/Psi-Erzeugung, niederenergetische Jets, geladene Ströme und als Gegenpunkt dazu reine Untergrund-Ereignisse.

1. Introduction

1.1. Physics at HERA

Most of the knowledge we have about the structure of matter was provided by scattering experiments. After the discovery of atoms and their constituents, electrons and nuclei, these nuclei were found to consist of protons and neutrons. At HERA, the investigations concentrate on the substructure of the proton.

Experimental facts have shown already in the sixties that there might be some point-like particles within protons and neutrons. Based on such observations the 'parton model' was developed. But still there are quite a number of properties of these partons one would like to measure experimentally, as it is the best test of a theory if some of its predictions can be verified by experiment.

This can today only be done by the assistance of huge machines, as particles have to be accelerated to immense energies. Such an accelerator named HERA (Hadron Elektron Ring-Anlage) has been built in Hamburg. In a more than 6 km long circular tunnel two different particle beam systems have been installed. One of them accelerates and stores 'pointlike' electrons with a maximal energy of 30 GeV, the other is filled with protons of up to 820 GeV that circulate in the opposite direction. These two systems work quite differently, as they have to struggle with different problems. For the electron beam, the energy-loss due to synchrotron radiation is a major problem. For the protons with their high momentum, specially strong magnetic fields were needed. They are generated by supraconducting coils and have a strength of 4.6 T. Both accelerators work at a frequency of 10.4 MHz which means that every 96 ns a particle bunch passes the detectors in each direction respectively. The time period of 96 ns is therefore the basic time interval of all the electronics at HERA and will be called 'one bunchcrossing' throughout this thesis.

The two beams are then brought to collision. A total center of mass energy of 314 GeV is at disposal for different particle reactions. The main points of interest are the following:

- The structure function of the proton. "What does it look like inside a proton?" The investigations concentrate on the structure function F_2 at low x and high Q^2, a kinematical range that has not been accessible to former experiments. This structure function would give additional information about the properties of

quarks and gluons, the suggested components of the proton.

- The total photoproduction cross section gives information about the proton structure as well as about the nature of photons.
- Gamma-gluon fusion: With such processes, the unstable quarks 's', 'c' and 'b' can be produced. This allows the study of particles as D-Mesons or the J/Psi.
- Charged current events where the weak interaction is realized by the exchange of a W^- vector boson.

A detailed introduction to the physics at HERA can be found in [3].

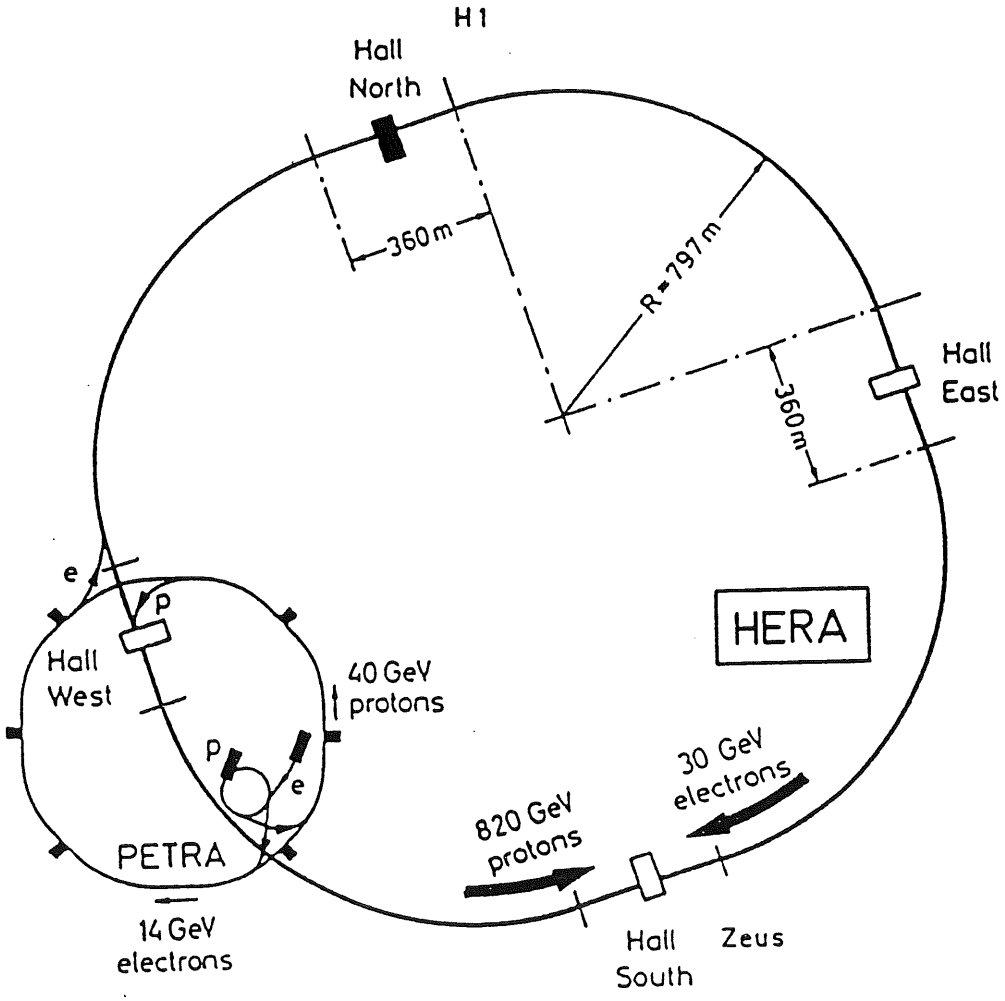

Fig 1.1. The HERA storage ring.

1.2. The H1 Detector

Large detectors called ZEUS and H1 [4] have been built around two of the four interaction zones of HERA. They are designed to measure the above described reactions at high accuracy. Trigger-electronics are a very important part of these experiments. As the HERA-accelerator works at a frequency of 10.4 MHz a physically interesting event could take place every 96 ns. The actual luminosity and the cross-sections of the investigated processes are however so small, that only a few events per second are probable. Therefore we have to distinguish between important and uninteresting data before the full readout of the detector starts. This is called a trigger-decision.

The H1-subsystems that will be referred to throughout this diploma thesis that describes the introduction of a new trigger system can be seen in Fig. 1.2.: A sophisticated tracking system includes cylindrical chambers around the interaction region (A) as well as planar chambers (B) in the 'forward direction' which is the direction of the protons and therefore the direction of the center of mass. The tracking system is composed of quite a number of different jet and multiwire proportional chambers. The latter are particularly important to us, as their fast available signals are the base of the z-vertex trigger.

The second system that matters in this context is the calorimeter of H1. It measures the energy of single particles as well as the energy of hadronic jets. A large range in azimutal angle from 4° (forward) up to 150 ° is covered by the Liquid Argon (LAr) calorimeter (D,E). It is described in chap. 2.1.1.

All the other subdetectors may be very interesting as well, but as they have no direct influence on the big ray trigger, they are not mentioned here.

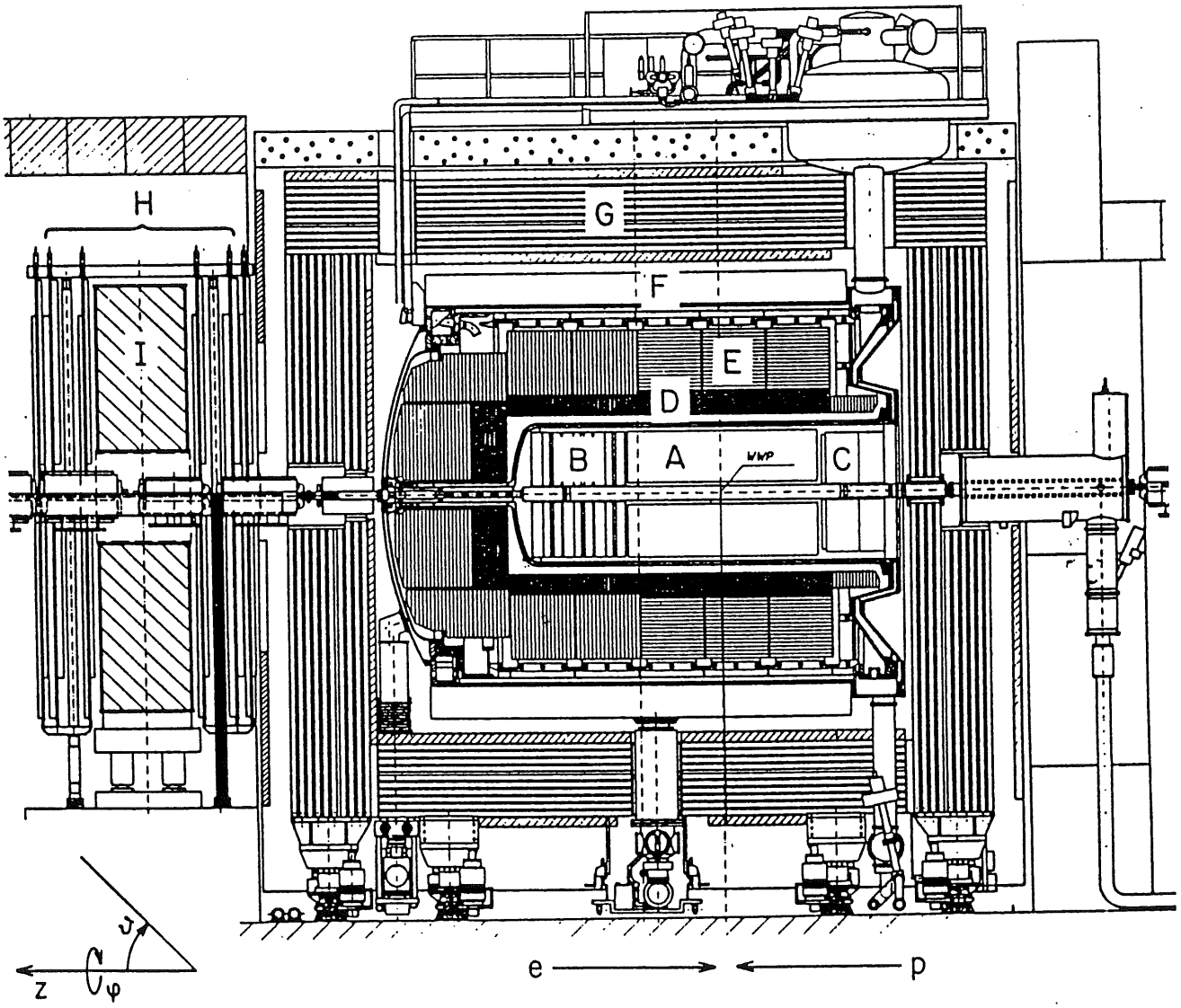

Fig. 1.2. Side view of the H1 detector. Protons enter from the right, electrons from the left side. The z-axis corresponds to the direction of the protons, θ measures the azimutal angle relative to the proton direction, φ is the polar angle. [4]

(A) central tracker (including CIP and COP) - (B) forward tracker (including FWPC0) - (C) BEMC (Backward Electromagnetic Calorimeter) - (D) electromagnetic and (E) hadronic layer of the Liquid Argon Calorimeter - (F) supraconducting coil - (G) instrumented iron yoke - (I) toroid magnet.

2. The First-Level Trigger

At HERA interactions of a proton with a gas-atom (despite the very sophisticated vacuum-system) or with the material of the beam-pipe are very common sources of particle-reactions. The electron-beam is also an important source of background, as it produces a lot of synchrotron-radiation that has to be distinguished form real electron-proton-scattering since these reactions are of no interest and should therefore be ignored.

The trigger of the H1 experiment is divided into four independent systems, called trigger levels (L1 - L4). The first level (L1) is directly connected to the detector and works therefore at the full input rate of 10.4 MHz. Only if the L1 trigger accepts an event, the information is communicated to the L2 system.

The L1 system should therefore be able to distinguish physically interesting events from background within a few microseconds, before the readout of the entire detector starts. This time is of course too short to calculate all the parameters of the event correctly. In consequence, the first level trigger is based on some typical values that can be calculated within relatively few steps. Every step of the analysis is realized in its own section of the hardware and executed within less than 96 ns. It can therefore be calculated at the same place for every bunchcrossing. In this way there is always data from several bunchcrossings processed at the same time at different steps of the calculation at different places. The entire information of all subdetectors of H1 is stored during this time in specific buffers called 'pipelines'. After about two or three microseconds the L1 trigger system has derived its result. Only if this answer is 'yes', the pipelines are stopped, which means that the information stored in these buffers is not dropped at the end of the lines as usual, but read by the central data acquisition system. No new information can be stored during the read-out. This setup is very useful to avoid dead-time: as long as there is no positive L1 decision, the detector works 100% dead-time free which means, that every bunchcrossing can be taken in consideration and no information is lost.

A positive trigger-signal of the L1 system is called 'L1-KEEP' as all the pipelines are stopped and their data is kept in memory by the central data acquisition system. During this readout ('primary dead time') the data is processed by the following trigger levels L2 and L3. As soon as the pipelines are read out the L1 system starts working again. The last level L4 is realized by a large 'computer-farm' - it works asynchronously and provides a first reconstruction of the events.

2.1. Calorimetric Triggers

2.1.1. The Liquid Argon Calorimeter

Calorimetric triggers are a quite important source of information. In the calorimeter particles are stopped by a large amount of material and the deposited energy is measured. At H1, the calorimeter is realized in a construction of lead- and steel-plates with liquid argon filled in between. An incoming particle interacts with the heavy nuclei of the lead or steel and produces a shower of secondary particles. As these particles reach the LAr-layer, they ionize the argon atoms. The freed electrons drift to the anode in the electric field produced by the high voltage applied to the gap. Here their signal is registered by the amplifiers of the readout. The final signal is approximately proportional to the energy of the primary particle or jet. However the system has a large electronic noise - short signals that appear without any particle passing the cell. This is a major problem for calorimetric triggers as it is nearly impossible to distinguish noise from 'real' signals in a short time.

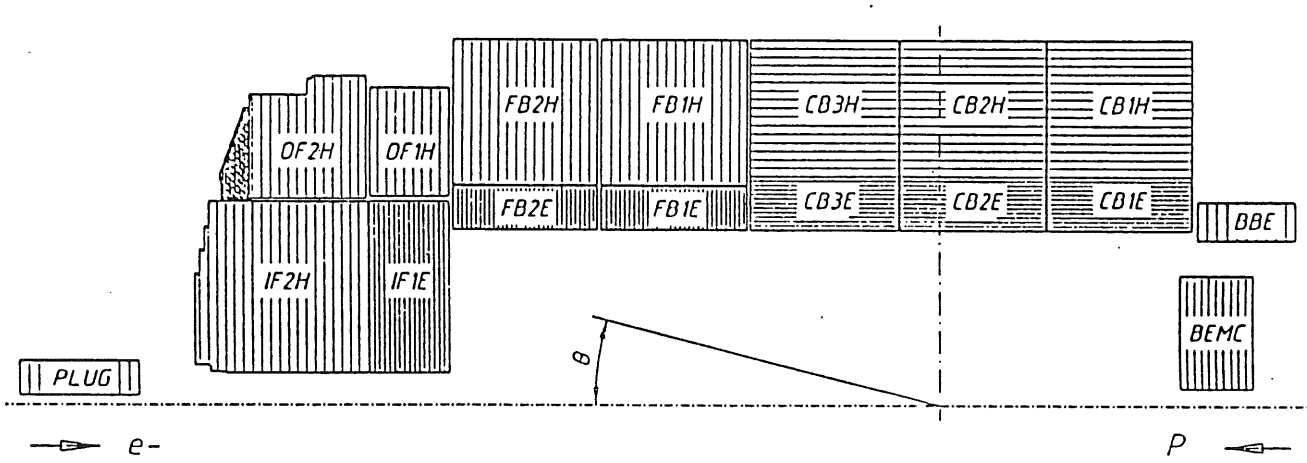

Fig. 2.1. Side view of the Liquid Argon Calorimeter. It consists of three 'central wheels', two 'forward wheels' and the 'inner forward region'.

The measurement of deposited energy is a good criterion to recognize physically interesting events such as deep inelastic scattering, where high-energy jets occur and a lot of secondary particles are produced. Its is on the other hand difficult to recognize events such as J/Psi-production with a decay of that particle into two electrons as there is only little energy deposited in the entire calorimeter by these two electrons. This problem might be solved partly by introducing the big ray trigger.

To understand the advantages of the big ray trigger, we have to discuss the structure of the LAr-electronics. Fig. 2.1. gives a good impression of the physical structure of the calorimeter with its 40000 cells. It is built from seven so-called 'wheels', cylindrical construction elements around the beam-axis. There is always an inner, ('electromagnetic'), and an outer ('hadronic') layer. In the inner layer the absorbing material is lead and electrons should be absorbed there totally by electromagnetic interaction. Heavy particles as hadrons pass this layer partly and are stopped mostly in the iron of the outer layer by strong interaction. Heavy leptons (muons) pass both layers nearly unhindered. The boundaries of the wheels are perpendicular to the axis and have therefore only little to do with the kinematics of particles coming from the interaction region. Therefore the structure of the trigger-logic is quite different.

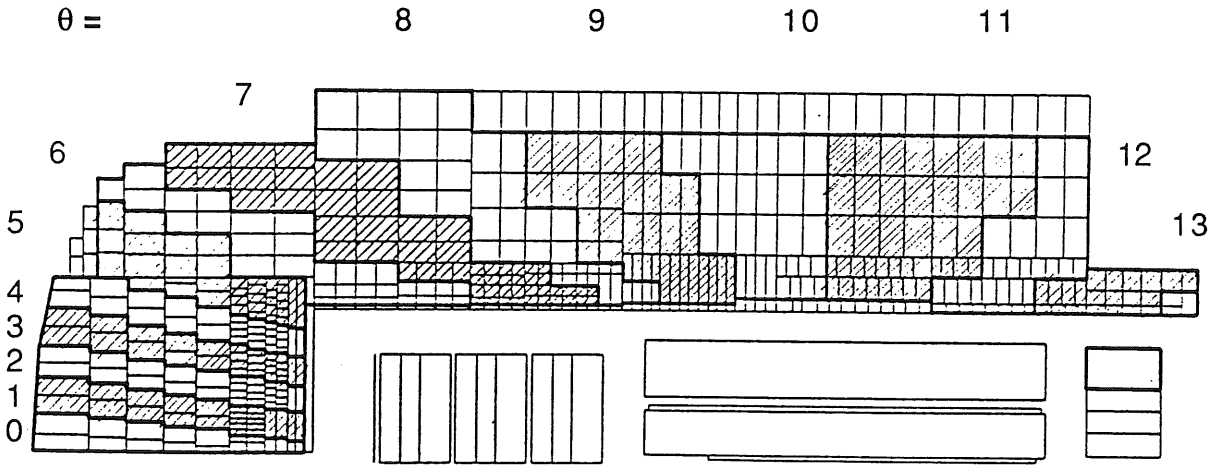

Fig 2.2. The readout cells of the LAr calorimeter are grouped to big towers, including cells of the electromagnetic and of the hadronic layer.

2.1.2. The LAr-Trigger

The geometrical structure of the LAr trigger can be seen in Fig. 2.2.: 14 groups of cells are formed in azimutal (θ) direction. In polar (ϕ) direction there is a further segmentation mostly 16-fold, for some θ segments 8- or 32-fold. In this way 240 groups of LAr-cells at different directions of the solid angle are formed. They are called big towers and include the electromagnetic layer as well as the hadronic. Big towers are made such, that they point relatively well to the interaction region and particles coming from there should therefore deposit all their energy in one single big tower. All the same, the energy of incoming particles is usually distributed over several big towers as a consequence of smearing effects. Such smearing effects result from the non-perfect geometry of the big towers and from the size of the secondary particle showers.

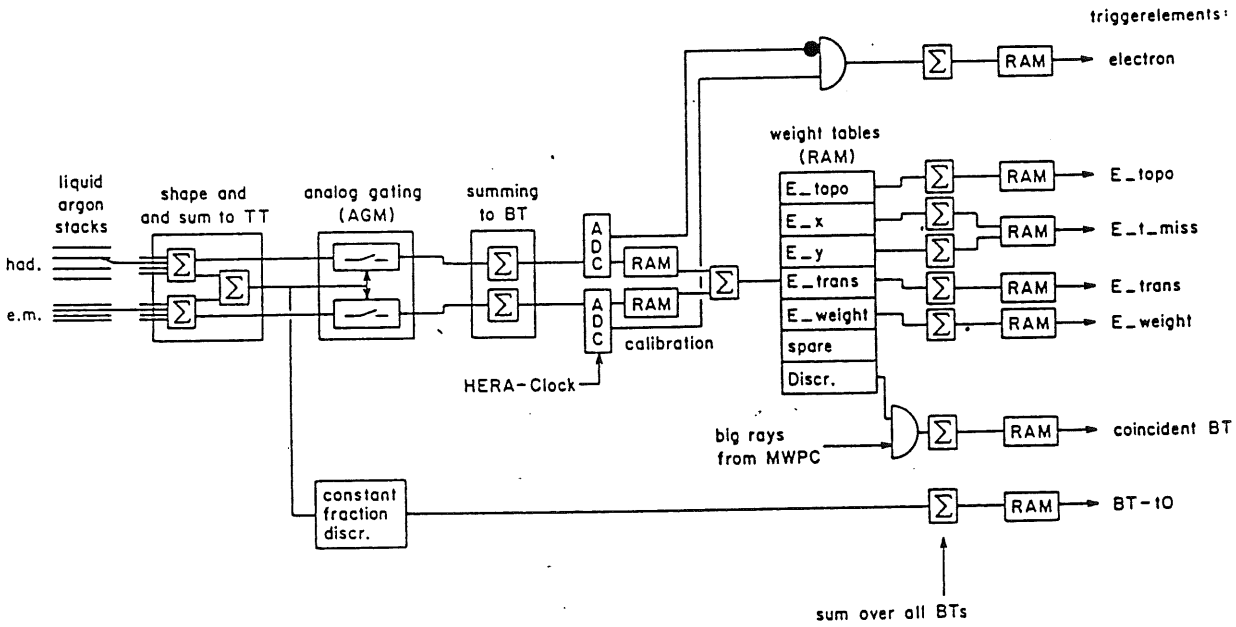

Fig 2.3. LAr trigger electronics. The last weight table is used to set the special big tower energy threshold 'S'. The appropriate value of this threshold will be discussed in chap. 5. At the coincidence after this discriminator tracking- and calorimetric- information is combined for the first time. In the following adder, the total number of validated big towers is calculated and by use of a look-up-table (RAM) two triggerbits according to two different thresholds are generated.

A schematic view of the LAr trigger electronics is given in Fig. 2.3.. The signals of a certain number of LAr-cells are summed up to the analog signal of one 'trigger tower'. It is rejected if it is below the 'AGM-threshold' ('Analog Gating Module'). Depending on the position in θ one, two or four trigger towers are then summed up to one big tower. Now the signals get digitized and calibrated by use of a look-up-table. These values are then spread out to a number of different trigger systems. Most of these triggers are uniquely based on the calorimetric information and calculate physically interesting values like transverse energy or missing transverse energy by use of further look-up-tables that contain geometrical information about each big tower.

2.1.3. The Big Ray Trigger

This new trigger is based on 'topological coincidences' between tracking triggers and the calorimeter. The idea behind is the following: As most of the particles should be detected by the proportional chamber systems, it is possible to extrapolate their tracks and therefore to find the big towers that absorb the energy of these particles. We have seen before, that electronic noise is the main problem of the LAr triggers. If we ask now for every big tower trigger energy exceeding a given threshold in coincidence with a track pointing to this big tower, we should get a quite selective criterion for real particle energy. This big ray trigger is the only L1 system that uses tracking information as well as calorimetric information.

For the practical realization of this idea we have to deal with big tower signals that pass further discriminators after they were digitized. They are then set in coincidence with the signals coming from the tracking triggers. In this way only big towers get validated that have registered an energy beyond the discriminator threshold and have at the same time a ray of the z-vertex- or forward-ray-trigger that is pointing in their direction. The number of these validated big towers is counted and if it exceeds a programmable threshold, a positive trigger signal is produced.

As mentioned earlier, we hope to be able in this way to detect a typical J/Psi event with that particle decaying into two electrons. When these electrons reach the calorimeter they do not deposit very much energy but they put it to a quite limited number of LAr-cells. Therefore we expect to find only one or two big towers per electron above the energy thresholds - if the electrons were also detected by the tracking-triggers, we ought to get two validated big towers. If on the other hand no

real particle has come from the interaction region there may still be quite a few big towers and big rays switched on by noise, but there is only a small chance that they lie in the same direction and are therefore usually not in coincidence. Hence background should be rejected in this way.

2.2. The z-Vertex Trigger [2]

2.2.1. Principle of Operation

The purpose of the z-vertex trigger is to find a common origin (vertex) of the particle tracks along the beam-axis (z-axis). This should be a good criterion to distinguish between electron-proton (ep)-collisions and background-events. The physically interesting ep-events take place in the interaction-region which is well defined by the size and the timing of the electron- and proton-bunches. It is about 40 cm long. Important sources of background-events such as beam-wall and beam-restgas collisions are in contrast quite regularly distributed along the beam-axis and so most of these events have a vertex outside the interaction-region.

The z-vertex trigger is based on the fast information available through six multiwire proportional chambers with cathode pad readout. These are: two layers of CIP (central inner proportional chamber), COP (central outer proportional chamber) and FWPC0, (first forward proportional chamber). CIP and COP are cylindrical chambers around the interaction-region. As the kinematics of the ep-collisions are very asymmetric, most of the events are boosted in 'the forward direction', (the direction of the protons). Therefore, three so called supermodules containing planar proportional- and drift-chambers are installed in the forward-direction. Their information is used in a special 'forward-ray-trigger'. The first layer of these forward supermodules is included in the z-vertex-trigger as well.

A particle originating from an ep-interaction normally passes four of these six chambers and therefore four pads should give a signal. Such a combination of four cathode-pads is called a 'ray'. The 'rayfinder' electronics is designed to find all these combinations of four pads that lie on a straight line. Every ray can be assigned to a certain z-position if one assumes that its origin is on the beam-axis. The interaction-region can therefore be mapped on a 16-bin histogram, where one entry is added for every ray found by the rayfinder-coincidences. Certainly there are also a lot of 'wrong' combinations of four pads that fire accidentally at the same

time, but these rays do not have a common origin on the beam-axis and should therefore be distributed randomly over the entire histogram. Accidental coincidences are reduced by the fact, that the chambers and the electronics have a 16-fold segmentation in polar- (ϕ-) direction. If a pad in one ϕ-segment has fired randomly, it cannot give a coincidence with a pad of a different segment. In addition a '3 of 4' option can be chosen for every ray, if a part of one chamber fails. Rays are then defined by a coincidence of the remaining three pads.

The histograms of the 16 ϕ segments are then summed up to get one final histogram, containing all the rays of all ϕ-segments. This histogram is then analyzed: the peak-height and -position are calculated, the total number of entries is summed up. These values are taken as input to a look-up-table on a 4MB ram card. At the end, one gets several quality bits for each bunchcrossing: Is there a significant peak? Is this peak just at the very end of the histogram? Does the histogram include only a small amount of entries? ...

2.2.2. Hardware Realization

Preamplifiers are already installed at the end of the chambers. They generate a differential analog signal that is transmitted by about 35 m long twisted-pair cables to the electronics-trailer.

The **Receiver Cards** are directly connected to these cables to discriminate and synchronize the signals with the HERA-Clock. This clock is generated by the accelerator-equipment and has a very stable phase relative to the electron- and proton-bunches. Therefore, this signal with its characteristic frequency of 10.4 MHz dominates the entire trigger. The digitized signals are then stored in special pipelines and at the same time fed to the rayfinder cards. The pipelines can be read by the central data acquisition if the L1-trigger-system accepts the event and sends the 'L1-KEEP' signal. As a special tool to debug and test the L1-triggers there are also two sets of buffers on these cards which can be taken as input instead of the signals from the discriminators. This allows to run a trigger with known input and in this way to compare its output with the expected values. A special signal is used to toggle between the two buffers. These computer-accessible buffers are also needed to load the z-vertex-trigger.

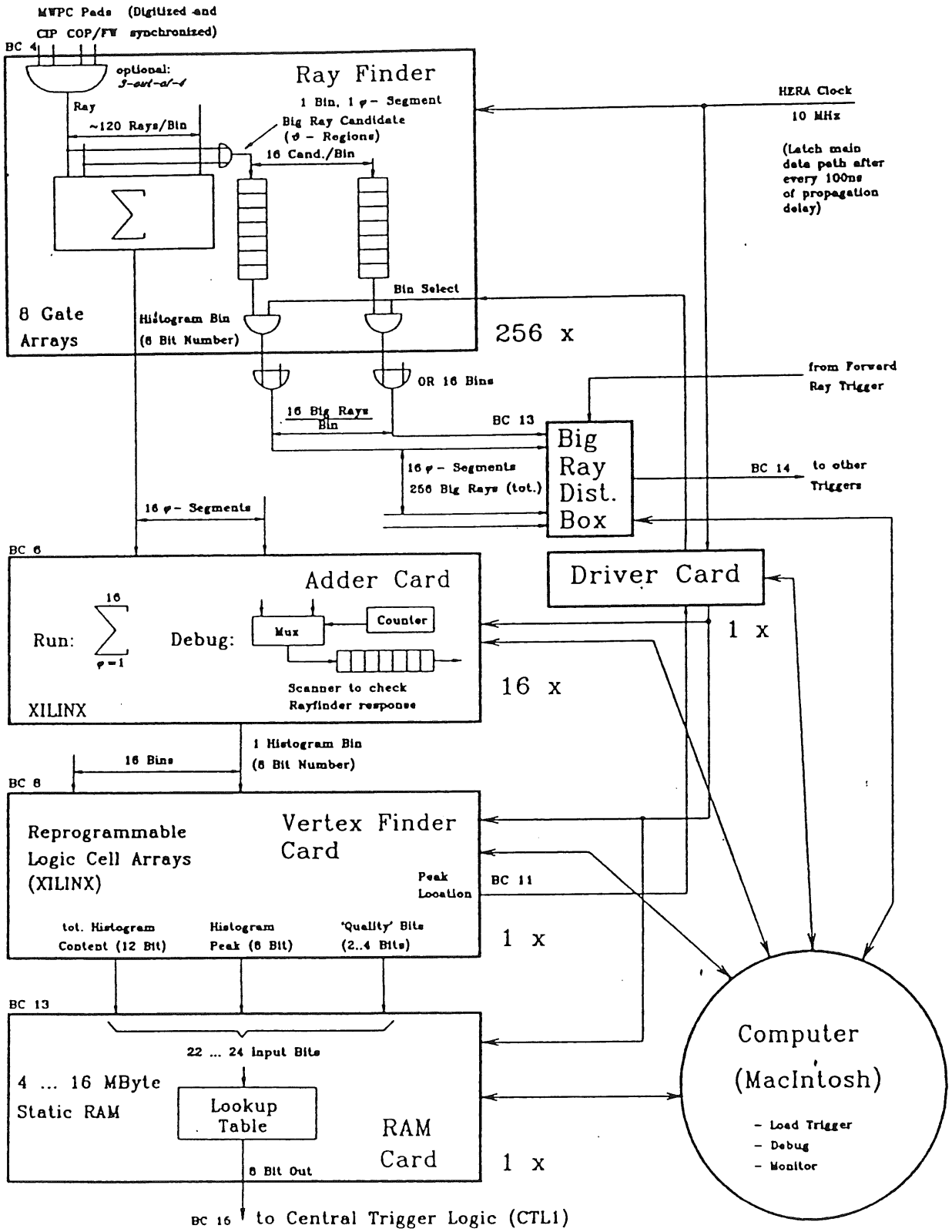

Fig 2.5. Block diagram of the z-vertex trigger. [2]

The design of the **Rayfinder Cards** was dominated by the strong demand of a parallel architecture. A total of 1920 input-signals have to be combined to more than 30 000 rays. This task is distributed over 256 printed circuit boards (PCB's) called rayfinder cards. These cards are first grouped by histogram-bin. Within such a group, which is situated in one half of a VME-rack, there are 16 PCB's, one for each ϕ-segment. Two rayfinder cards share one slot. The 16 cards of one bin are identical, as there is no geometrical difference between different ϕ-segments. They are unique for every bin as it turned out to be impossible to find a common wiring between the coincidences on the 'rayfinder gate arrays' and the input connectors on the backplane for all the geometrically different bins.

The coincidences that define the rays are realized in the **Rayfinder Gate Arrays** [1] (Fig. 2.6.) These 'application specific integrated circuits' were designed uniquely for this purpose. They have a complex inner structure; some important details will be described later in chap. 4.3. In the so-called 'INPUT'-block, the coincidences corresponding to the rays are realized. A second block, the 'ADDER', counts the total number of active rays (0-31) and generates a 5-bit pattern corresponding to that number. The found rays are at the same time input to the programmable 'OR', the principal component used in this diploma thesis. This previously unused block allows, to form an OR of every ray available at up to five different output pins. At the end of the OR-block there is a pipeline installed with a programmable length between 1 and 8 steps. A further important block is called 'CONFIGURATION' and contains the memory of the gate arrays. This memory is necessary to store information about the programming of the OR and to point out the rays with '3 of 4'-option selected.

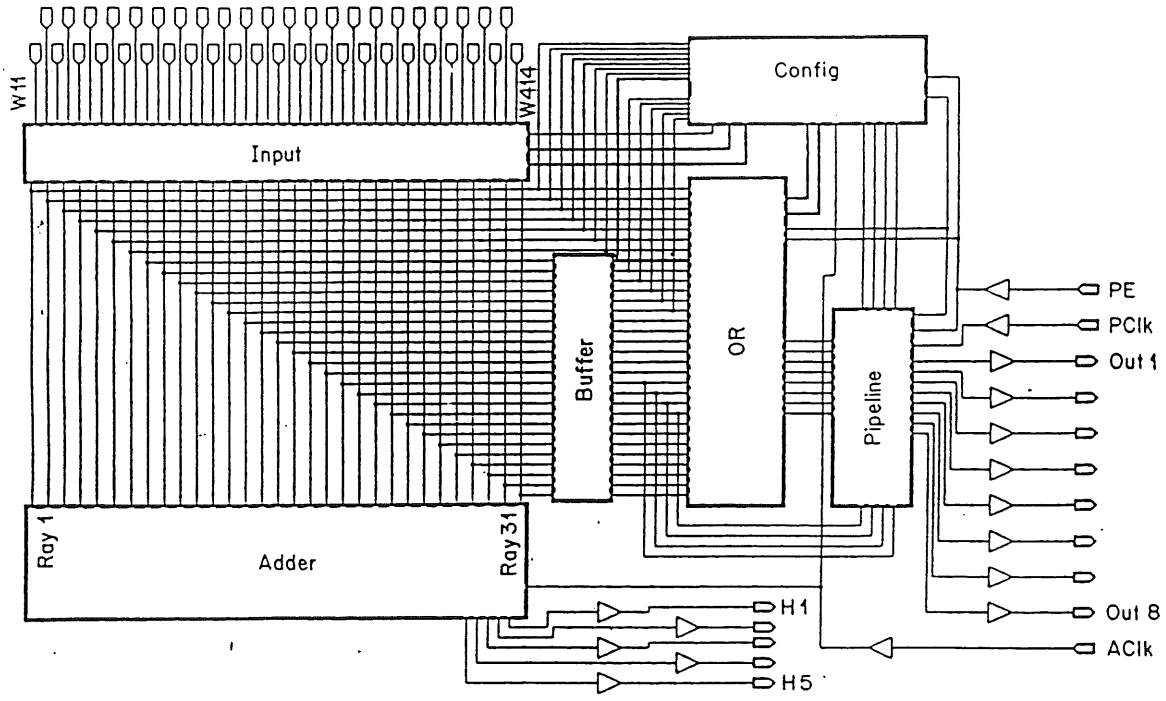

Fig. 2.6. Block diagram of the 'rayfinder gate array'. [1]

On each rayfinder card, there are six or seven such gate arrays, the 'raybuilder gate arrays', which build about 120 rays. Two additional 'big ray gate arrays' per card were put to use during this work. Their input-pins are connected to the output of the pipelines of the 'raybuilder gate arrays'. They are set to 'direct mode' which means that every input-pin is directly assigned to a ray and no coincidences are required. In this way the output of the pipelines on the raybuilder gate arrays is directly fed to the input of the OR on the big ray gate arrays and can then be matched again to one of the pipelines of these gate arrays. These two additional gate arrays are necessary because the rays of one bin are distributed more or less randomly over six or seven gate arrays and have to be combined to 16 big rays. Therefore it has to be possible again to form an OR of the output of the 'raybuilder gate arrays' to the final 16 big ray signals (see Fig. 4.2.). The output, two times 8-bit, of the pipelines of these 'big ray gate arrays' is enabled only when the bin select signal is active. On the backplanes of the rayfinder cards there is a wired OR of all the big ray signals of all bins of the same ϕ-segment. By use of the bin select signals, we can enable the output of a selection of gate arrays and the final big ray signals will be the 'OR' of the selected bins (e.g. only the peak-bin and its neighbors).

Now the signals are fed from the z-vertex trigger to the **Big Ray Distribution Box** (BRDB). This crate is designed to do the correct mapping of the big rays to the big towers of the LAr-trigger. Input are the big rays of the z-vertex-trigger as well as those reconstructed by the forward ray trigger. Some programmable registers allow to choose how the overlap-section of these two systems is handled and whether the big rays found in one ϕ-segment should switch on the big towers of the neighboring ϕ-segments as well or not. In the BRDB every ϕ-segment corresponds to one card.

The output of the adders of the raybuilder gate arrays is first fed into an 8-bit adder on the rayfinder card. This information is then transmitted to the **Adder Cards**, where the content of one bin is calculated by adding all the corresponding ϕ-segments. The result is fed to the **Vertex Finder Card** where the contents of all bins are compared in order to find the location and the height of the peak of the histogram. On this card some of the quality-bits and the total content of the histogram are calculated as well. Adder and vertex finder cards are realized nearly identically. The heart of these cards are four Xilinx Logic Cell Arrays. The complete adder- and comparator-logic is placed inside these programmable chips. This realization allows an update of the logic whenever there is a new function required. This was very helpful, since there are now different versions of the Xilinx configuration in use. (see 3.3.)

The **Look-up-Table (Ram Card)** is the last element of the z-vertex-trigger. Peak-height and total content of the histogram are input to this 4 megabyte random access memory (RAM). These values are interpreted as addresses and point to a certain register of the memory. At this place the information is stored, whether these two characteristics of the input histogram correspond to a significant vertex (i.e. whether the peak is much higher than the average of the histogram). A look-up-table has been chosen because the explicit calculation of the level of significance could not be done within a few logical steps and would therefore have consumed too much time. There are two different significance-bits available corresponding to different restrictions to the peak.

2.3. Central Trigger

The trigger systems described above and some other ones not described here generate a total of 128 different signals, called L1 trigger elements. As none of them is selective enough by itself, a system is required that produces nearly any desirable cocktail of coincidences and anticoincidences of these different trigger elements. This is realized by the 'central trigger'. It can generate 128 different combinations of trigger elements, called subtriggers. These subtriggers are not connected to any subsystem of the detector any more but carry the specific signature of a certain class of physical events. If any of these subtriggers accepts an event, the L1-KEEP signal is sent out to all the subsystems of the detector and the readout starts. At the same time, the higher level triggers get the information they need to process the event.

L1 triggers should occur at a total rate of about 1-5 kHz. This rate is to be compared to its input of 10.4 MHz, whereby one has to take care of the fact that background occurs only at a rate of about 50 kHz and for most of the bunchcrossings, there is no activity in the detector at all.

3. Geometrical Considerations

As already mentioned, the LAr calorimeter is divided into 240 big towers covering different sections of the solid angle. The geometry of these groups of cells is by far not perfectly pointing and as shown in Fig. 3.1., a particle produces a shower of secondary particles that is about as large as one big tower. On the other hand, the ensemble of all possible particle tracks that switch on the same pads of the proportional chambers and therefore the same rays of the z-vertex trigger has only a limited geometrical accuracy as well. The assignment from rays to big towers must take care of these geometrical imperfections. For every big tower, a 'big ray' was defined, which is the ensemble of all the rays pointing to this big tower. This chapter will show how this was done within the constraints of the hardware.

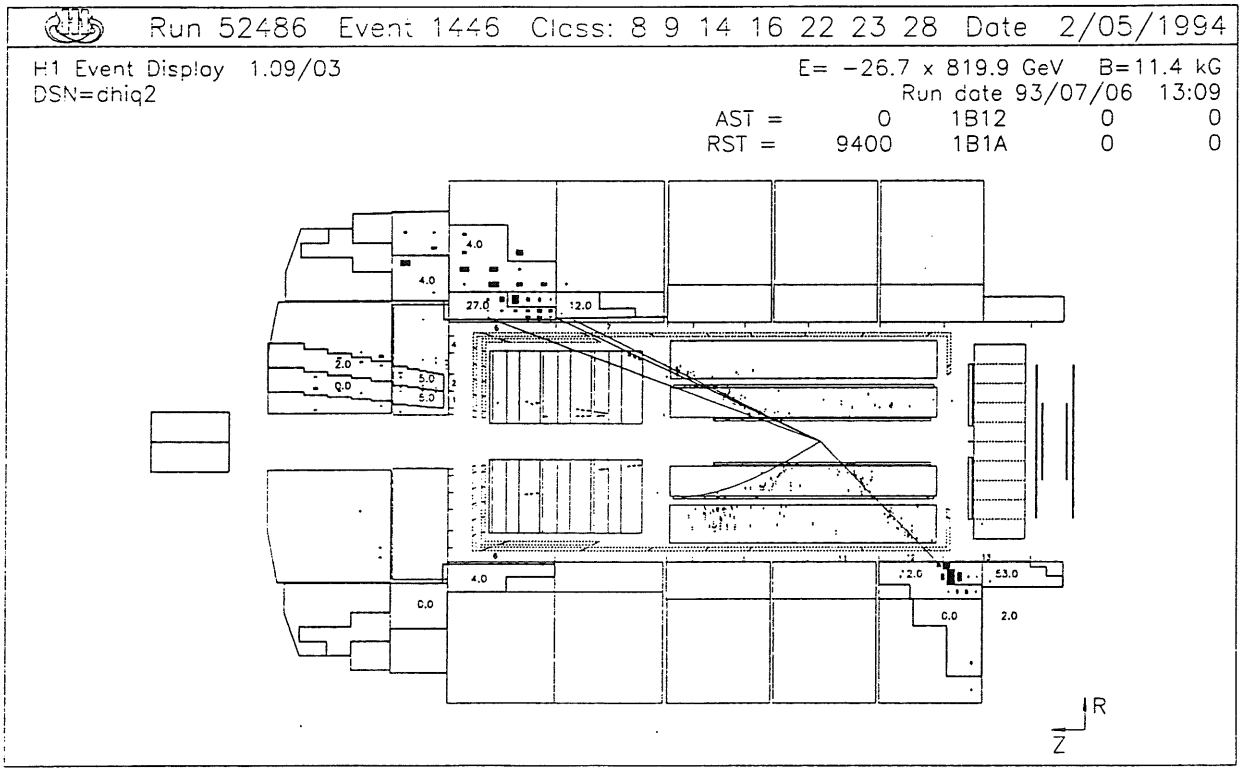

Fig. 3.1. In a typical 'High Q^2' - event the energy of the particles is not concentrated in one single big tower per particle, but smeared over a large region.

3.1. Overlap in Azimutal (θ) Angle

As the big towers point aproximately to the interaction-point of the ep-reactions, particle tracks should (neglecting smearing effects) usually not cross more than one single big tower. We therefore decided to base our definition of 'ray number n points to big tower number m' on whether the particle tracks reach the inner surface of the LAr-system in the range of that big tower or not. A range in r (forward) and z (barrel) was therefore attributed to every ray and to every big tower as shown in Fig. 3.2. and 3.3. It was then easy to define the big rays as the ensemble of all the rays with ranges that intersect with the range of the according big tower.

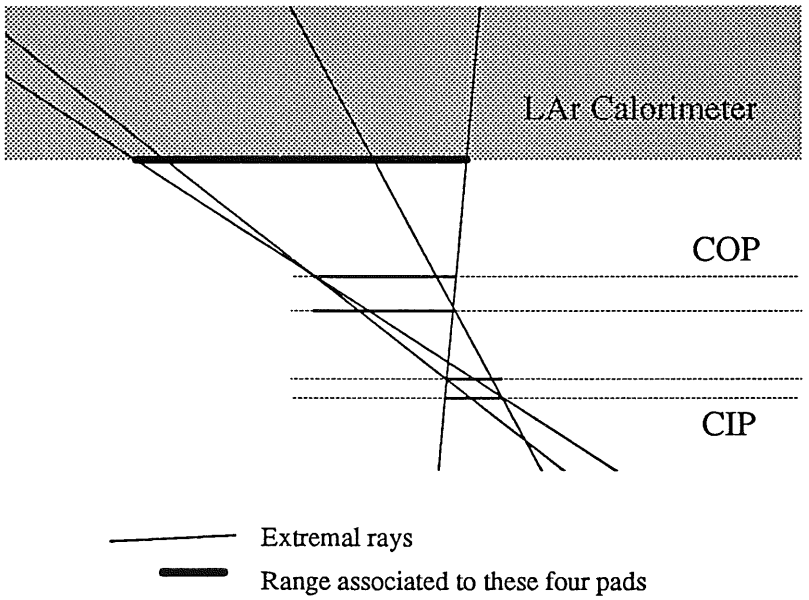

Fig. 3.2. Construction of the lines defining the range of one ray on the inner surface of the LAr calorimeter.

3.1.1. Definition of z-Vertex Rays

A coincidence of four proportional chamber pads is called a ray. As the pads have a finite size, there is quite a number of possible particle tracks that can switch on the same ray. The endpoints on the inner surface of the calorimeter of all these tracks associated to one ray define the range we are interested in. This range was calculated by a computer program for every ray. Fig. 3.2. shows that one certainly finds the extrema of this range if all lines passing through the ends of two pads are

calculated. All the other possible tracks through the same four pads end between these four points. As a simplification, the curvature of the particle tracks due to the magnetic field and effects at the border of the pads are neglected here.

3.1.2. Definition of the Big Rays

The proper definition of the non-perfect geometry of the big towers and the particle showers would have forced us to solve a lot of secondary problems, e.g. the size of a shower depends strongly on the energy of the primary particle. We therefore decided to define an 'overlap factor' and to find its appropriate value by analyzing the simulated behavior of the trigger. The definition of this factor will be given here, the results of the simulation are shown in chap. 5.2.5. and 5.2.6.

Our definition of the big towers was based on their inner endpoints. This simplification should be quite accurate since the big towers point to the interaction region. The calculation was based on the ABTG databank which contains the average value of cos (θ) for every big tower. The endpoints of every big tower were defined just in the middle between its center and the centers of the neighbors. The range attributed to this big tower was then enlarged by use of the overlap factor:

$$D = D_0 * (1 + F * 100)$$

where D_0 is half the distance from the center of the big tower to the center of the neighbor and D is the width of the attributed range with an overlap of F [%]. (Fig. 3.3.).

As a convention, big rays and big towers are numbered from 0 ('forward') to 13 ('backward') within every ϕ-segment (see Fig. 2.2., Tab. 3.1.).

#θ	mean value of θ [°]	region	attributed range [mm]
0	θ_m = 4.60	forward ->	r= 175.6 - 297.9
1	θ_m = 6.97	forward ->	r= 297.9 - 429.8
2	θ_m = 9.66	forward ->	r= 429.8 - 572.7
3	θ_m = 12.37	forward ->	r= 572.7 - 711.6
4	θ_m = 14.82	forward ->	r= 711.6 - 876.9
5	θ_m = 18.37	forward ->	r= 876.9 - 1153.7
6	θ_m = 24.46	barrel ->	z= 1950.5 - 2652.0
7	θ_m = 31.68	barrel ->	z= 1365.0 - 1950.5
8	θ_m = 42.93	barrel ->	z= 847.5 - 1365.0
9	θ_m = 58.72	barrel ->	z= 387.7 - 847.5
10	θ_m = 80.40	barrel ->	z= -87.1 - 387.7
11	θ_m = 109.18	barrel ->	z= -610.8 - -87.1
12	θ_m = 131.67	barrel ->	z= -1202.7 - -610.8
13	θ_m = 146.62	barrel ->	z= -2142.1 - -1202.7

Tab 3.1. Geometrical properties of the big towers. A range in radial (axial) direction is attributed to the big towers in the forward (barrel) region. The overlap factor has been set to 0%.

3.2. The Overlap in Polar (φ) Direction

The problem of the size of the particle showers in the calorimeter occurs in φ as well as in θ. In addition, because of the strong magnetic field of about 1.2 T along the beam axis, the assumption of straight tracks does not hold for the transverse components, in particular for low energy particles.

In the hardware, θ- and φ-overlap is treated differently, too. In θ the rays are attached to the big towers by use of the programmable OR on the rayfinder gate arrays in a very flexible and accurate way. In φ however, we have to deal with the 16-fold segmentation of the proportional chamber and the z-vertex trigger electronics as well as with the 8-, 16- and 32-fold segmentation of the LAr big towers. A special tool is therefore foreseen in the big ray distribution box, which is the only place where the big ray signals of different φ-segments pass a common

crate. A 16-bit mask (the last two bits are unused) can be applied to decide for every θ whether the big rays should include only rays of one φ-segment or those of the neighboring segements as well. The limited flexibility of this solution is a direct consequence of the φ-segmentation of the proportional chambers, and can therefore not easily be improved.

A further problem arises from the inhomogeneous segmentation of the LAr system. In the case of a 32-fold segmentation in φ, the coincidences of two big towers are connected to the same big ray signal coming from the BRDB. In the case of a 8-fold segmentation, the situation is reversed: two signals from the BRDB are assigned to the same big tower. Performing this function requires additional logic. In this case (θ=13) only the odd numbered φ segments are connected to the LAr trigger. If the 'validate φ neighbors' bit is set for this θ segment the problem is more or less solved: every big ray of the tracking system enables at least the signal of the LAr big tower it is pointing to and no information gets lost. This option has therefore always to be set. Refering to 'φ neighbors off' in the following therefore means that the φ neighbors are only validated in the θ=13 segment.

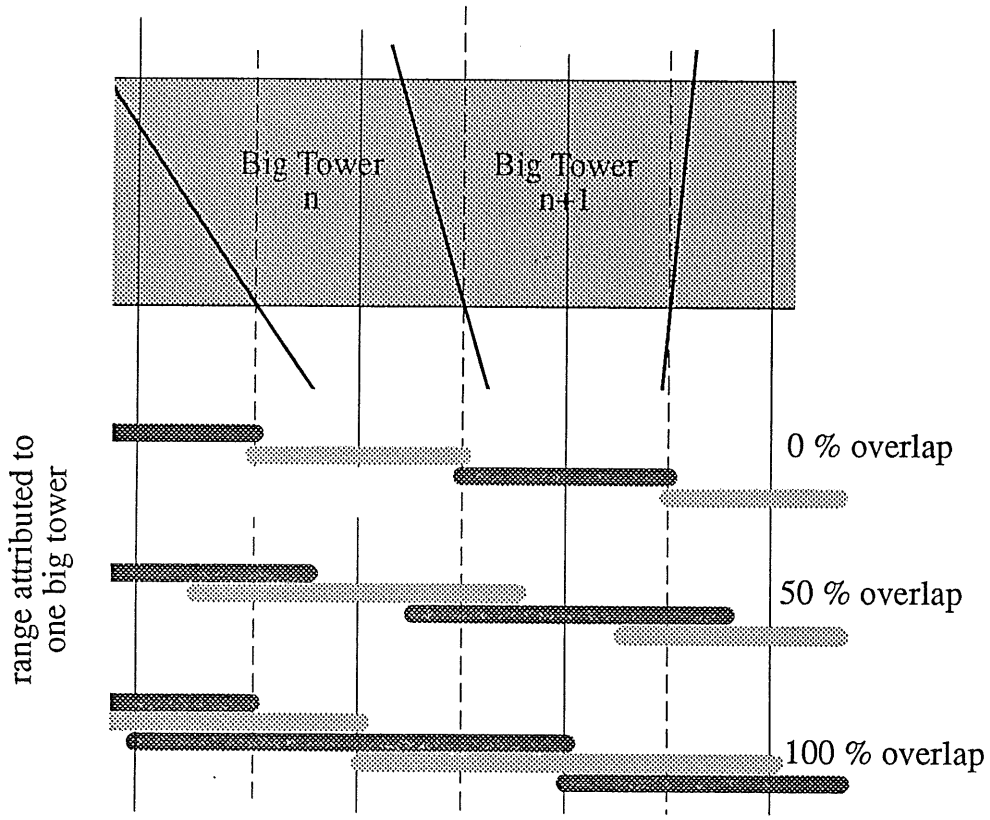

Fig. 3.3. The range attributed to one big tower is enlarged by the overlap factor. For 100% overlap, every ray enables at least 2 big towers.

3.3. The Origin of the Validated Rays in the z-Vertex Histogram

As mentioned before, there are also accidental or 'wrong' coincidences of four pads in the z-vertex trigger. It would not make sense to validate big towers just because they are in a line with such rays that have no physical meaning. Therefore we would like to have an instrument to distinguish between 'right' and 'wrong' rays. It is obvious, that rays originating from the vertex of a particle interaction have a much better chance to correspond to a real particle track than those coming from a different point. This distinction can partly be realized by use of the 'Bin Select' signal. This signal is fed to all the 'big ray gate arrays' of one bin and serves there as 'Output Enable' signal, which means that there is no output of the pipeline of these chips, unless this signal is active. The bin select signal is computer accessible and already used for the programming of the gate arrays. Its input can be switched from the computer to some output pins of the Xilinx chips on the vertex finder cards. The circuits in the Xilinx programmable logic cell arrays can easily be extended such that the bin select signal of the peak-bin is set active and all the other ones remain passive. Another possibility is, to set active the 'bin select' of the peak and its direct neighbors ('Peak +/-1') or even of the next two bins on each side ('Peak +/-2'). In consequence, only rays originating from these selected bins are validated and no ray from outside the peak-region can switch on a big ray.

The geometrical considerations that determined the size of the pads of CIP and COP were such, that the uncertainties of the track position within the pads yield to a resolution of the histogram of about one bin. Therefore, it is reasonable to consider all the rays with an origin at the peak or its direct neighbors as valid.

The results of some proves of this argument will be given in chapter 5.

4. Hardware Realization

4.1. Data Flow

The introduction of big rays involves a quite complex data flow as we will see in this chapter. A schematic view is given in Fig. 4.1. Most of this data flow can be divided into a Macintosh and a UNIX part. The Macintosh computer is being used to steer the hardware via a VME-Interface, the UNIX machines have been used for off-line tasks.

Starting point of the data flow is a file called 'ALL.PRN' that was set up by Stefan Eichenberger when he realized the z-vertex trigger. This ASCII-file contains the information about all rays - where they are located in the gate arrays and which pads are associated to them. A first new program called 'PadGARay' reads this file and generates a list 'Rays' containing the same information in a format that is better readable. This list is, together with the 'ABTG' databank (see chap. 3.1.2.), input to the program called 'BigRayDef'. Geometrical constants of the detector (proportional chambers and LAr system) are stored in the program itself, the overlap factor and a unique version-number (date) have to be given interactively. The geometrical operations calculated by this program have already been explained in chapter 3.1.

As output three different files with the given version number in their name are generated. 'CTRC_.....' is a databank already known by the detector simulation software 'H1_sim'. It contains one row for every ray formed by 'CIP' and 'COP' pads. Pad numbers, the histogram-bin and the range of big rays, to which a ray is attached to, are given in that row. 'CTRF_..' similarly contains the rays built by two pads from 'CIP' and 'FWPC0', respectively. A third file called 'Pointed_By_...' contains a matrix with one column for every big ray and one row for every ray. '1' signifies that the ray is element of this big ray, '0' that it is not.

'Pointed_By' is input to the program called 'Combination' that reads the file 'ConnectGA_GA' containing information about the cabling on the PCBs between 'ray builder gate arrays' and 'big ray gate arrays' as well. The program 'Combination' then tries to find a programming of the gate arrays that achieves all the assignments required by 'Pointed_By'. An overview of the chosen algorithm will be given in chapter 4.2. The program generates as output a series of files stored in a directory called 'ProgBits_...' and the raylist 'ALLB.PRN_...'. The latter is similar to the starting file 'ALL.PRN' but contains in addition the information about the programmable 'OR'. The 'ProgBits' files also contain this program for the 'OR' but in

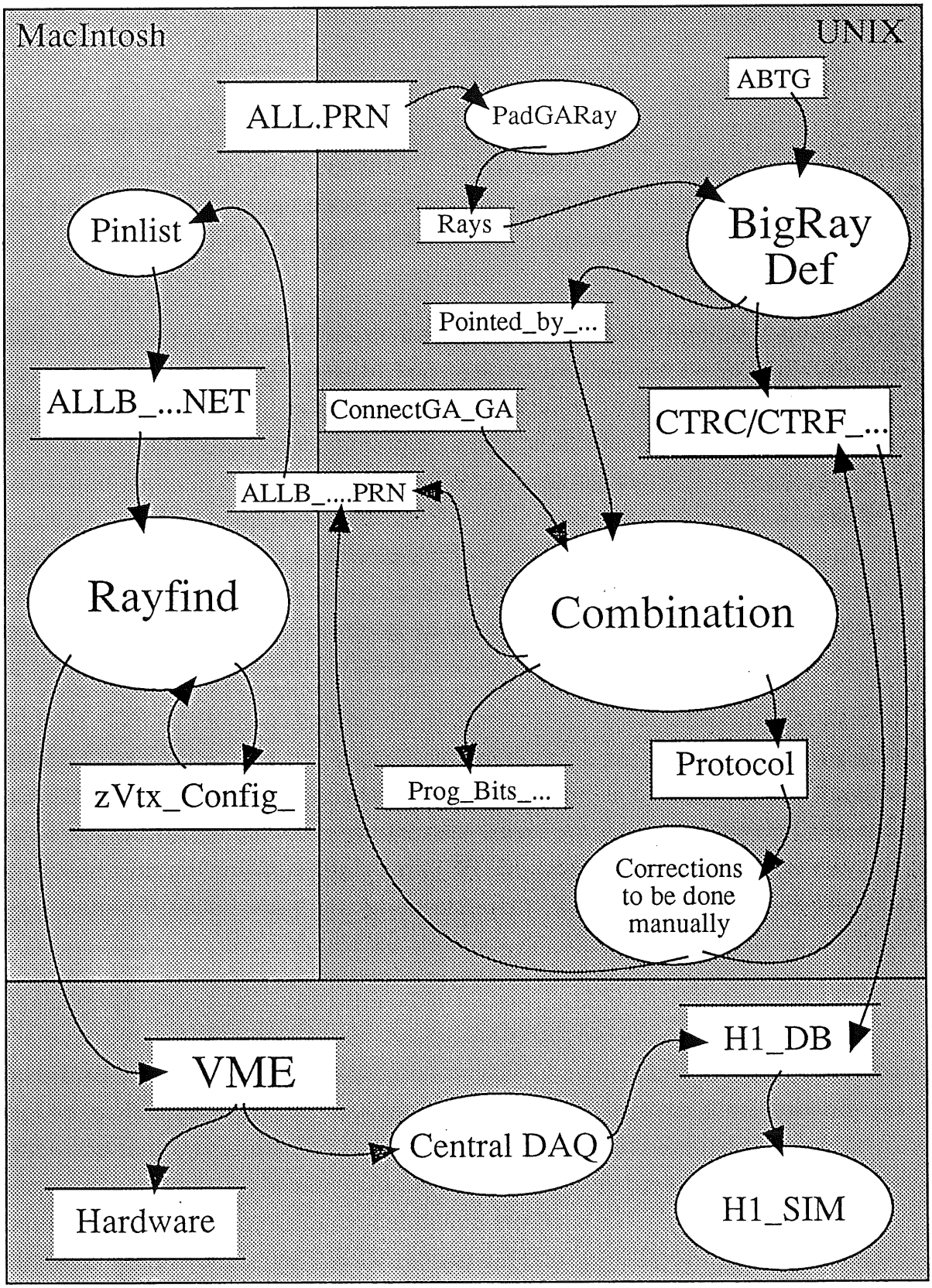

Fig. 4.1. Dataflow for the programming of the big ray trigger. The individual blocks are described in the text.

a 'dump-like' form - every register of a gate array gets one line with its eight bits. These files have been very useful to test the program but have no importance for the data flow any more.

As alternatives to the geometrical definitions shown in chapter 3.1. have been proposed, the entire task of the gate array programming was split into two independent programs, 'BigRayDef' and 'Combination'. If it will turn out later, that a better definition of the big rays than the one executed by the program 'BigRayDef' is needed, it will be easy to generate the same format of output files and to use 'Combination' without any additional work.

However, an unpleasant detail needs to be mentioned: as the program achieves only about 99.8 % of all the required assignments 'ray to big ray', there are some corrections of 'CTRC', 'CTRF' and 'ALLB.PRN' to be done manually as will be explained in chap. 4.2.

The ASCII-file 'ALLB.PRN' is transferred to the MacIntosh computer and translated to a binary file called 'ALLB.NET' by the program 'Pinlist'. All the necessary preparations are finished now and the program 'Rayfind' that is designed to steer all the hardware accesses can be started. (The data flow of the Xilinx-programs is omitted here and will be shown in chap. 4.4.)

The 'Rayfind' program takes additional information like the name of the netlist to be used (version name!) out of a file called 'zVtx-Config-...' and includes a large amount of cabling-information as stored in the file 'ConnectGA_GA'. Via the VME interface, information is now transferred to the hardware of the trigger (programming of gate arrays and Xilinx chips ...) and into a memory, which will be read by the central data acquisition system ('DAQ') of the H1 experiment and written to the official data banks of the corresponding run (version number...).

4.2. The Generation of the Gate Array Programs

It has been shown in chap. 3.1. how the assignment of rays to big rays was calculated. The problem was then to realize these geometrical requirements with the already existing hardware.

Up to seven raybuilder gate arrays per rayfinder card generate up to 31 rays each. These are to be combined into an OR for the corresponding big rays which are

represented by the two times eight bits of the big ray gate array pipelines. (See Fig. 4.2.) In between lie the programmable ORs of both types of gate arrays and the connections on the PCB.

The technical constraints were the followings:

- Every ray can only be fed to 3 to 5 given pipelines out of 8 (see [1]: Tab. 3.3.).
- Not every pipeline of a 'raybuilder' has a connection to a big ray gate array.
- Some pipelines are connected to both big ray gate arrays.

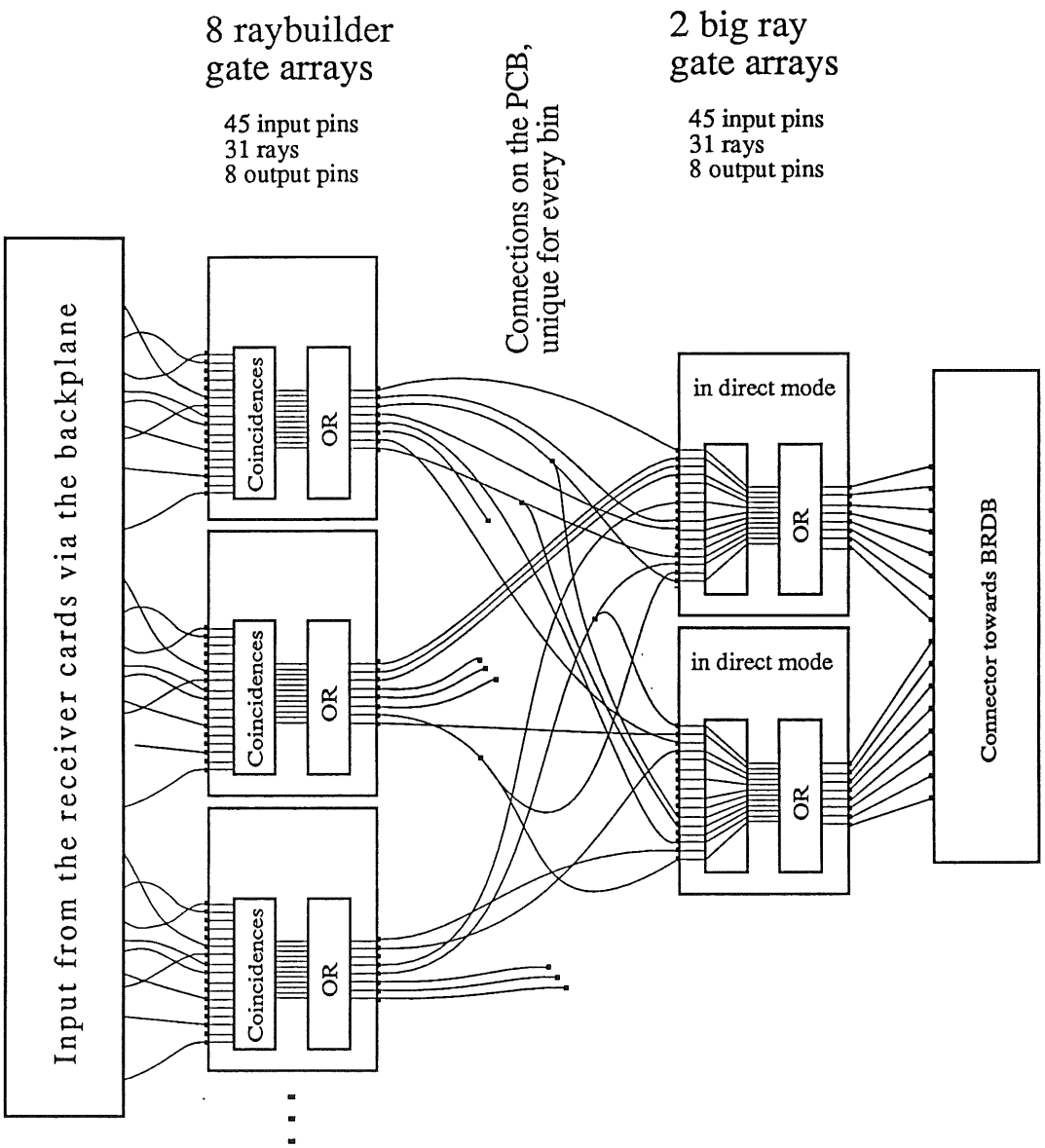

Fig. 4.2. Schematic view of the technical constraints to the programming of the OR on the 7 + 2 gate arrays.

It was not clear at the beginning, whether all the required assignments could be realized or not. The results of some studies showed, that there are in fact certain situations, where this is impossible. To ensure that the optimal programming of the gate arrays was found, one could have tried all the possible combinations of the 155 bits of the programmable OR of each gate array. However an estimate showed that this procedure would require more than a million years of CPU-time of the workstation used. Since a diploma thesis is supposed to be finished within one year, a faster algorithm had to be developed. An overview of the program 'Combination' finally used is given in the following.

It is advisable to start considerations at the big ray end. For each big ray the program checks for all the rays of the corresponding big ray gate array whether they can be fed to it, and if yes, what raybuilder pipeline they originate from. These pipelines have again a certain number of rays that can be fed to them: 'normal rays of the z-vertex trigger'. The program counts then how many of them are elements of the big ray we started with. Having done so for all the possible assignments 'raybuilder pipeline to big ray' the program chooses the attachment that is able to realize the largest number of assignments 'ray to big ray'. The connection used on the PCB is labeled, the bits for the gate arrays are prepared and the assignments 'ray to big ray' realized are taken out of the list of tasks. Now, a new cycle of this procedure starts until there can be no assignment realized any more. However, this usually does not mean that there is no one left to be done...

The whole procedure has to be done independently for every bin since the PCB's are unique for every bin while there are no differences between different ϕ-sectors.

The philosophy of the program is "always fetch the best opportunity". This yields certainly to a good but probably not to the best global solution. It turned out to be very useful to try solutions that lie close to the above described one as well. This is done in the following way: instead of the criterion described above, the number of realized assignments multiplied with a random number between 0.8 and 1.2 is to be maximal, for that assignment 'raybuilder pipeline to big ray' is choosen. It is therefore possible to execute a loop over the entire assignment procedure and, due to these random factors, there is every time a different result to be expected. This procedure could be repeated until a perfect programming of the gate arrays (which realizes all the required assignments) is found. As there are certain cases where we are convinced that not all the required assignments can be realized, this would turn out to be an ever-lasting loop and therefore, after a certain number of loops (usually 500), the condition of the loop is set to 'realize all but one

assignments' and after twice this number, the condition is simplified again to 'all but two' and so on. This procedure has turned out to be quite efficient and fast.

As mentioned before, there are always certain assignments 'ray to big ray' that cannot be realized by the hardware. As the response of the trigger is always tested by the corresponding simulation program based on the 'CTRC' and 'CTRF' database, these inefficiencies have to be simulated as well. The databases therefore have to be corrected. As this was done only once, it has not been automated but was executed 'manually' in the following way:

'Combination' identifies the non-realized assignments on standard output by ray (bin, gate array, ray) and big ray. One has to find the pads associated with that ray first, an information that can easily be found in the file 'Rays'. There the task is made complicate, since the pad-numbering in this file starts at one. In addition the chamber number times 1000 is added to the pad numbers (CIP inner=1, CIP outer=2, COP=3,4, FWPC0=5,6). Therefore, one has now to decrement these numbers by one and take them 'mod 1000' to get the usual zero-based numbers! With this information one can then do the needed modifications of 'CTRC/CTRF'. A specially intricate problem occurs, if a ray is e.g. associated to big rays #5 to #7 and it turns out that there was no possibility found to realize the connection to big ray #6. In this case, one has to set the range in 'CTRC/CTRF' to #5 to #5 and to delete in 'ALLB.PRN' the row that would set the bit that ORes this ray to big tower #7!

4.3. 'Rayfinder' Gate Arrays

4.3.1. The Programmable OR of the Gate Arrays

The structure of the Gate Arrays has already been shown in chap. 2.2.2. However, we have to look at some details more closely now. Fig. 4.3. gives a schematic view of all the steering signals within a gate array.

A first important switch is controlled by the 'Mode Control' bit. By use of it, the entire 'Input' block can be bypassed. Thus the 31 'rays' within the gate array are not associated to a coincidence of 4 input pins any more, but to one single pin. This mode is used for the big ray gate arrays, as their input pins are connected to the output of the pipelines of the raybuilder gate arrays and requiring such 4 fold coincidences would make it impossible to transmit these signals to the OR of the big ray gate arrays.

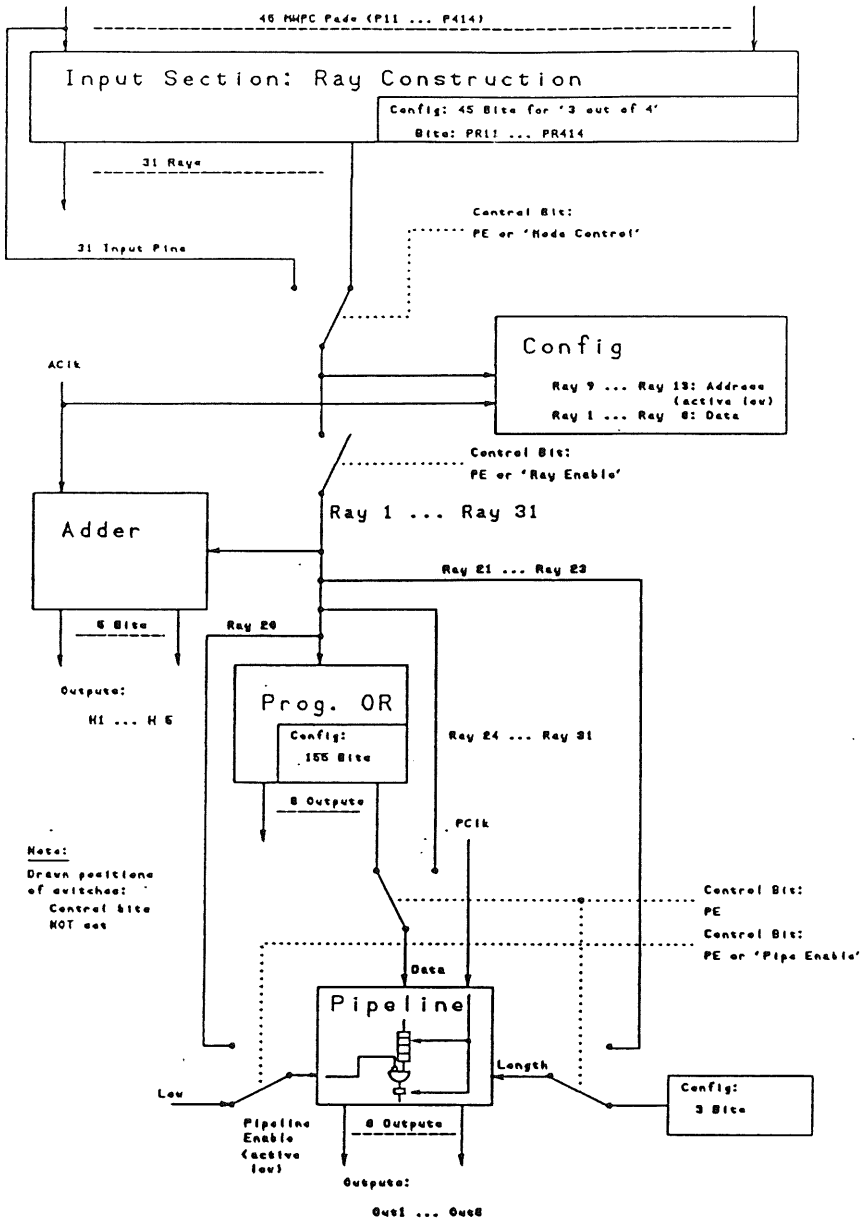

Fig. 4.3. Flow diagram of the gate array [1]

The external signal called 'Program Enable' has some important effects: the gate array is set to direct mode and programming of the 'CONFIGURATION' memory is enabled whereby five rays are interpreted as addresses and eight rays are used as data lines. A last switch is controlled either by the 'Pipe Enable' bit of the memory or by the 'Program Enable' signal. If this bit is not set or if one is programming, the output of the pipeline is validated and therefore fed to the output pins of the gate arrays. This configuration is selected in all the raybuilder gate arrays. In the big ray gate arrays however the 'pipe enable' bit is set. Therefore, the output of their pipelines is only validated, if ray #20 of these gate arrays is active (=low!). The pins

corresponding to ray #20 of the big ray gate arrays are connected on the PCBs to the 'bin select' signals. The origin of these signals has been described in chapter 2.3.: they can be switched on and off by the logic on the Xilinx chips and are such set active for the peak-bin and its neighbors. (The inverters of the signals are realized on the vertex finder card, it is active high in the Xilinx chips and active low on the rayfinder cards.) Therefore, only the 'big ray' signals of these validated gate arrays reach the wired OR on the backplane of the rayfinder crates and thus the BRDB. The 'bin select' signal is also used during the programming procedure, but then assigned to the 'program enable' signal.

One might wonder, why pipelines are used, since they cause an additional delay of the signals. There are two reasons why this makes sense. On one hand we have to wait until the peak of the histogram is found and the 'bin select' signal is generated. On the other hand, this delay is necessary as the trigger signals from the LAr big towers are available only relatively late due to the limited rise time of the calorimeter signals.

4.3.2. Programming of the Gate Arrays

The new procedure to load the big ray gate arrays will be explained after giving a review of the loading cycle of the raybuilders.

At first the 'program enable' signal of the gate array, one wants to program, has to be set. This is done by first switching on the corresponding 'bin select' signal by the steering computer. In a second step we have to choose the appropriate gate array. This is done using a 4 bit multiplexer on each rayfinder PCB. These multiplexers are usually set to an illegal gate array number, lets say 15. On the desired rayfinder card, it is now set to the number of the gate array we want to program. The 'bin select' signal is therefore transferred to the chip we want to program where it is interpreted as 'program enable'. Now, we can access the memory of this gate array in the following way: certain 'rays' (9..13) are interpreted as addresses, others (1..8) as the data to be stored at that place. The memory covers 30 registers of 8 bits each. The problem of this procedure is, that the 'rays' of the gate arrays are not directly computer-accessible. They can only be steered by a test-pattern that is loaded to the receiver cards (see chap. 2.2.2.) and fed from there to the raybuilder gate arrays. These are in direct mode and therefore interpret certain single input pads as rays, a not very straightforward, but nevertheless reliable method.

If we now want to load a big ray gate array, the procedure gets even more

complicated, as these chips are not connected to the receiver cards. We now have to channel the program information through the raybuilders and to feed it this way to the big ray gate arrays. For this purpose, we have to load a special setting to all raybuilders: 'direct mode' has to be set, the 'pipe enable' bit must be low. In addition, we have to program the OR such that every pipeline gets the information of just one ray and can therefore be accessed by the data transferred from the computer to a receiver card. As the output of the pipelines is transmitted to the two big ray gate arrays, we have thus found a method to transfer any desirable data to the memory of them, as soon as they are set to 'program enable' mode. It is obvious, that the raybuilder gate arrays have to be loaded again after this procedure with their appropriate data.

4.3.3. Debugging Tools

The entire logic of the z-Vertex trigger is a very complex system. Thus, a quite sophisticated computer simulation of the hardware is needed to make the detection of hardware defects possible. This program has to indicate all the signals that are to be expected at any pin within the hardware as well as at the output of the trigger. Such a tool has already been realized in the Macintosh program 'Rayfind' but some upgrades were necessary to simulate the newly introduced functions as well. As the Macintosh only gets the information stored in the file 'ALLB.NET' the principles of this program are closely related to the hardware e.g. big rays are calculated by using the data about the programmable OR that is really loaded to the gate arrays. A second simulation program runs off-line and is based on the 'CTRC/CTRF' databases and therefore closer to the geometrical considerations. A comparison of these programs turned out to be very useful to detect bugs in the calculation of the programming of the gate arrays by the program 'Combination'.

As a further debugging tool the 'Test Pattern Run' was invented. A series of randomized proportional chamber signals are generated by the computer and transferred to the receiver cards. In this way, an event is simulated artificially and a positive trigger signal ('non-empty histogram') is produced by the z-vertex trigger. If the central data acquisition system is running, this trigger can start the readout of all the pipelines one is interested in. These are usually the receiver cards, the BRDB and the corresponding pipelines of the LAr trigger as well as the output of the z-vertex trigger (trigger elements, histogram). These 'artificial events' can be generated at a rate of about 3-4 Hz and can therefore provide a statistically significant test of the involved hardware.

However, there is no such handy instrument to check the synchronization between the proportional chamber trigger and the calorimetric system, as there is no possibility to generate common test-pulses. Only the analysis of real particles (cosmics or beam) causing signals in both systems could provide a test of this synchronization.

4.4. The Xilinx Programming

The layout of the 'Peak Finder' logic cells arrays has already been discussed in [2]. Only relatively little change was needed now to implement the newly required functions on these chips.

It has to be mentioned here, that if there are several peaks with the same height in the histogram, they are all flagged as 'peak bin' and none of them is preferred or neglected in any way.

These new functions could be designed graphically by use of a commercial program. The implementation of these graphical layouts on the Xilinx chips and the creation of the corresponding files was done more or less automatically by a standard software.

4.5. The Big Ray Distribution Box

This crate has been designed and installed by the Orsay group LAL (Laboratoire d'accelerateur lineaire, Paris) in 1993 but had not been used until now. This 'box' is the interface between the tracking triggers and the trigger electronics of the LAr system. It consists of 16 cards, one for each ϕ segment of the tracking system. As the LAr-trigger requires input sorted by azimutal (θ)-angle, there is a complex wire-wrapping on the backplane of this box.

A schematic view of the cards is given in Fig. 4.5. They take the big ray signals of z-vertex- and forward ray trigger as input. As the forward ray trigger is based uniquely on the information of the forward proportional chambers, it covers only a part of the azimuthal range and there are therefore only 7 big rays in θ. The incoming signals are latched with individually adjustable clock phases and then stored in separate pipelines. These are used to test the correct performance of the z-vertex- and forward ray trigger during all data taking periods and some special tests as described in chap. 4.3.3. A first logic block called 'CONFIG' is used to determine how to combine the signals of the two tracking triggers in their overlap region (θ = 0 - 6). All the four possible combinations as 'only z-Vertex', 'only forward', 'z-vertex AND forward' and 'z-vertex OR forward' are possible and can be chosen by use of a special Macintosh program called 'TRC'. For the θ segments #7 to #13 the signals from the z-vertex trigger are used directly. At this level, the signals can be seen by the experimentalist as they are fed to LED's. This simple control instrument provided a very useful service when we started to use the BRDB. Later on we used the data read from the pipelines mentioned before and the LED's were not that important any more.

Via the backplane, these signals are transmitted to the neighboring cards i. e. to the electronics corresponding to the neighboring ϕ segments. In the same way, every card gets the big ray pattern of its two neighbors. The block 'TOPOLOGY' is fed with these signals and realizes the 'enable ϕ neighbors' function: a programmable 16 bit pattern is used to determine for each θ segment whether the neighbors in ϕ should be allowed to switch on this big ray or not. It is very important that this can be done for every θ segment separately as we have seen, because this function must always be set for the θ segments with only eight fold ϕ segmentation in the LAr system (chap. 3.2.). It seems though that for the other segments it will usually be switched off to reduce the noise rate. After a further delay differential signals are generated and transmitted by twisted pair cables to the LAr system.

Before the signals get merged with those of the neighboring ϕ segments, they are also fed to the 'J/Psi' block and to the PQZP crate, where the big ray information is available to the level 2 and 3 systems.

Besides the LAr-big ray trigger that is object of this thesis, two other big ray trigger elements should be mentioned here:

- The so called 'J/Psi' trigger: In this system the pattern of active big rays is projected in θ direction. As a J/Psi with low transverse momentum decays into two identical particles (electrons, muons), these events should be recognized by their caracteristical two active ϕ segments, one situated in opposition of the other.
- The 'backward big ray' trigger: This trigger element is active, whenever any big ray of the θ segments #11 to #13 is active. These big rays correspond to large scattering angles and thus to a high momentum transfer.

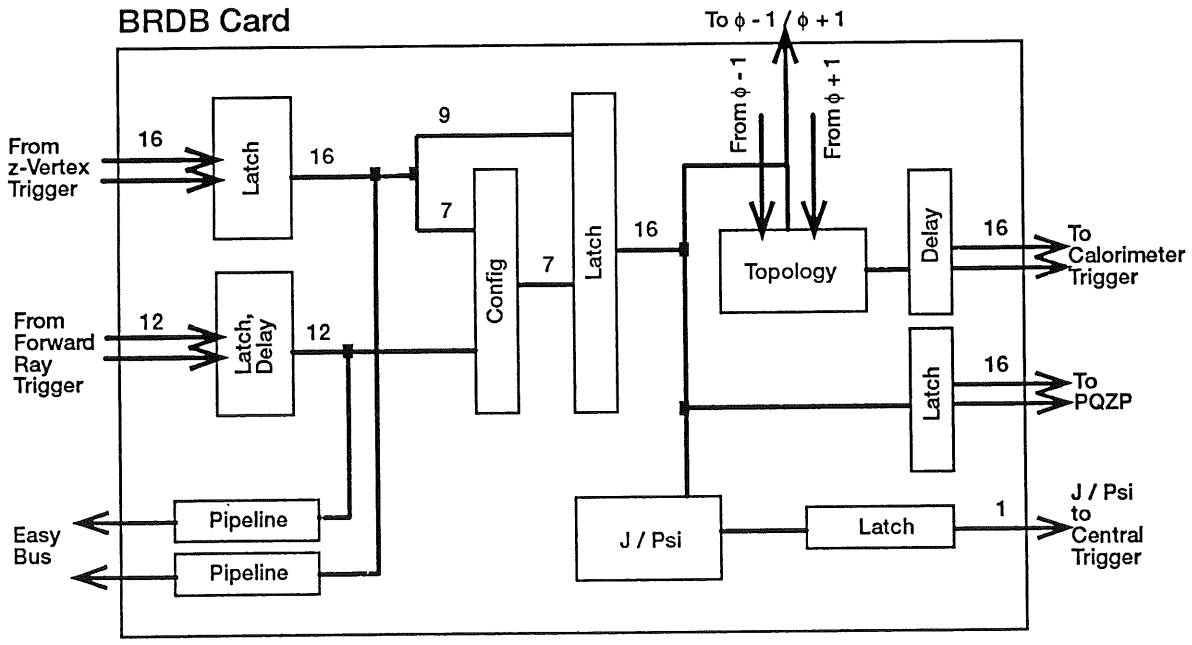

Fig. 4.5. Block diagram of the BRDB - cards.

5. Analysis of the Trigger Behavior

5.1. Some Examples

A first method to test the gate array programming was based on the Macintosh program described in chap. 4.3.3. Since there is a special tool to load the MWPC response of any real event of the 1993 data taking period as a test pattern to the computer we can calculate the expected response of the big ray distribution box as well. It is then possible to compare the pattern of active big rays in ϕ and θ with the real measured energy of the LAr system. However, this procedure is quite expensive in CPU time because the program algorithm follows exactly the steps of the hardware setup. All the technical constraints of the electronic components add an unnecessary expense. Therefore, no attempt has been made to automate the comparison of these two patterns.

Much more attention has been paid to the possibilities provided by the off-line simulation software. These programs are designed to control the behavior of all the H1 subsystems during the data taking and had therefore to be adapted by the experts in charge to the new trigger function. As only the final results are compared with the hardware, these programs use much faster algorithms, which do not pay attention to the technical setup of the hardware. A very positive effect of the upgrade of these programs to our investigation was the possibility to simulate the behavior of the big ray trigger based on real data from 1993 very fast thus allowing the analysis of a statistically significant number of events. A very successful example of such a comparison is given in Fig. 5.1. The big ray pattern is simulated by use of the MWPC signals whereby only z-vertex rays have been taken in consideration. Big rays from the forward ray trigger have been suppressed. Since big rays should point to deposited real particle energy and not to noise of the LAr trigger, the plotted energies of the big towers do not correspond to the values determined by the trigger electronics but to a simulation on base of the much more accurate values of the event readout. The energy of all the readout cells that are element of one big tower were summed up and this value was then interpreted as real big tower energy. The value of the threshold was subtracted and all the big towers that still had a positive energy (i.e. which had an effective energy above this threshold) would have passed the discriminator and if the attributed big ray had been on, this big tower would have been validated. In figure 5.1., the 'enable ϕ neighbors' function was assumed to be on. A fact to be taken specially care of is,

that for θ = 13 there is only an eight fold ϕ segmentation of the LAr trigger towers. Therefore only the odd ϕ segments correspond to a big tower while the even ϕ segments have no meaning at all.

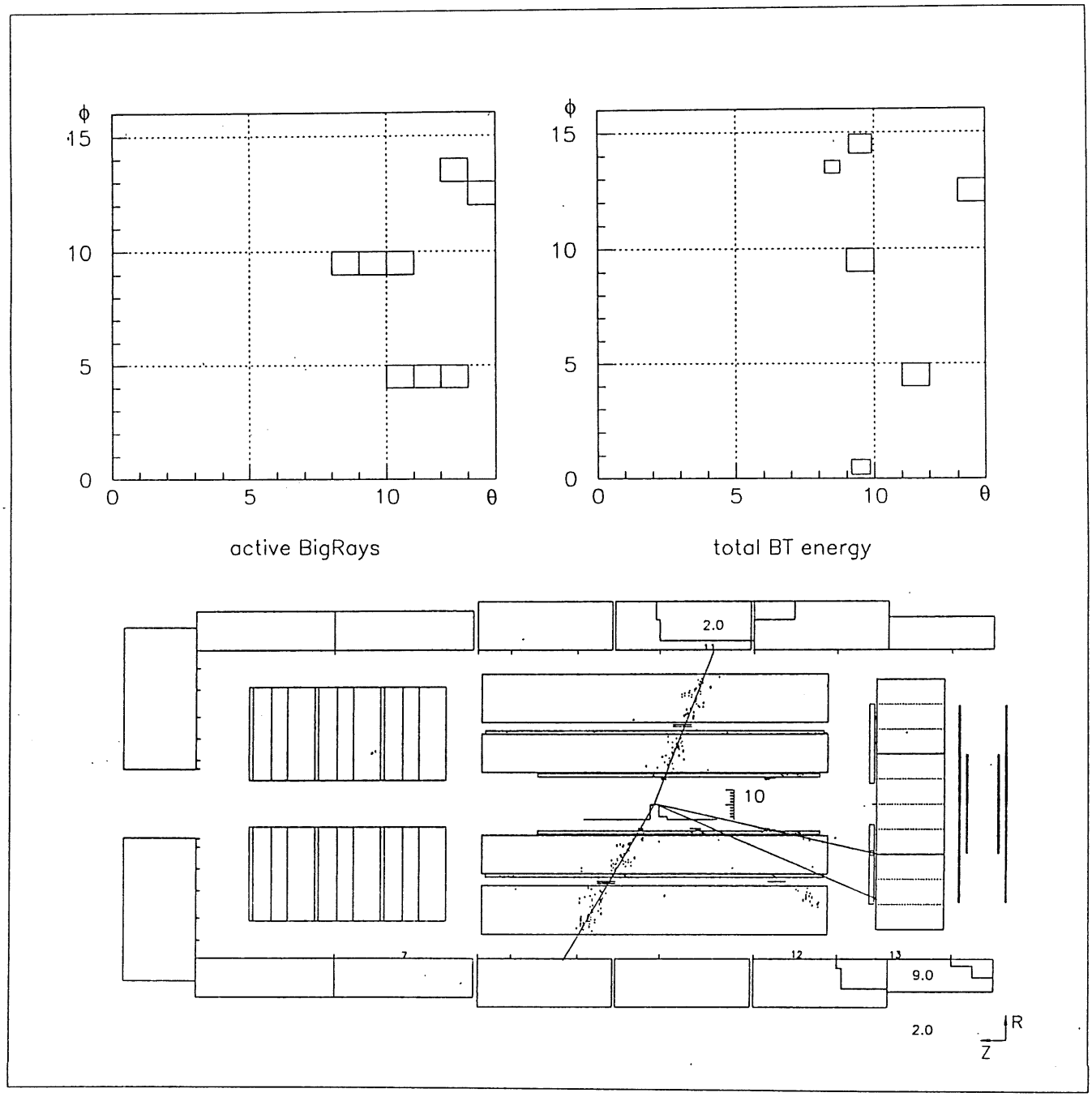

Fig. 5.1. Simulation of the big ray trigger: the active big rays correspond perfectly to the real particle energy and to the reconstructed tracks. The '3 out of 4' option has been selected for the ray pointing to ϕ=13, θ=13 (event display: lower right). The tracks to the BEMC have no influence to the big ray trigger since only the LAr calorimeter is included.

5.2. Simulation of Efficiencies for Different Classes of Events

The above described procedure was very useful to get a first impression of the response of the big ray trigger. It was on the other hand not designed to give a statistically significant answer to the questions about how to use this trigger in order to detect specific classes of physical events. In this chapter, it will be shown that some answers to these questions could be given. In doing so we have to caution that no attempt has been made to trace possible systematical errors. Furthermore specially the rates for the simulated background should be interpreted only as very rough estimates.

To get an overview about the use of this new trigger, three classes of physically interesting events were examined:

- Gamma-gluon fusion of J/Psi decaying afterwards into an electron and a positron.
- Low energy jets generated in photoproduction processes.
- Neutral current induced events with a high momentum transfer ('High Q^2') as they were observed in the 1993 data sample. This class of events has already been studied carefully otherwise because it is possible to use the scattered electron signal in the backward electromagnetic calorimeter in the trigger.
- Charged current events however are much more difficult to trigger since the incident electron is converted to a neutrino and escapes undetected. We simulated such events by 'deleting' the identified electron of the neutral current events i.e. by taking all the energy that was assumed to be deposited by this electron out of the data. The remaining event should correspond to a charged current exchange. Since the cross section to produce such events is very small due to the high mass of the virtual propagator (W^-), and designing a trigger for them is very difficult because of the undetectable lepton, the recognition of these events could be a task for the big ray trigger.

Some special runs with a trigger that accepted every event with minimal activity in the detector were taken in 1993 to get information about the background. The results of these runs were used to give an estimate of the background rates of this new trigger. This is quite important as the efficiencies to physics events are only relevant, if the trigger at the same time is able to reduce the background rate down to an acceptable value. Background signals due to random coincidences between big rays and real big tower energy could in a first step be calculated easily. In

addition, we tried to get an estimate of the complete noise rate, including electronic noise of the LAr system as well. This could not be done just by analyzing the 1993 data because the settings of the LAr trigger have been changed in winter 93/94 and the noise situation was therefore expected to be completely different. Three procedures were developed to estimate these rates: two of them combined data of a first cosmics run in April 1994 with the background run 1993 mentioned above. The third procedure was based on the results of a first run triggered by big rays on May 25th 1994.

5.2.1. Efficiencies for Physics Classes

The events used to calculate the expected trigger efficiencies have been selected out of the 1993 data by different groups of physicists doing analysis on these classes of physics. Therefore, this method of simulation gives not the efficiency for all the events of the corresponding class but only for those that were already accepted by a different trigger. It is therefore possible, that the effective efficiencies lie below the calculated values as it is to be expected that the events rejected by the already used triggers are also more difficult to be recognized by the big ray trigger.

As described in 5.1. the number of validated big towers with real energy above a given threshold was calculated for every event. This procedure leads to a certain underestimation of the efficiencies of the big ray trigger since some big rays could validate noise-signals of the LAr and the total number of validated big towers could therefore be increased for some of the events randomly. The number of events that satisfied the condition "n or more big towers validated" was then calculated for every n from 0 to 5 and divided by the total number of events in the sample. This ratio was interpreted as trigger efficiency. The errors were calculated by use of the formula for binomial distributions. The same procedure was used to calculate the beam related background rate due to validated real big tower energy. (The efficiency was then multiplied with the total rate of the background run.) Coincidences with some other tracking triggers could be required in addition to simulate possible future subtriggers. We included z-vertex quality bits and the so called DCrϕ trigger, a L1 system that triggers on bent tracks in the projection to the plane rectangular to the beam pipe. A combination with further calorimetric triggers was not possible as there would again arise the problem of the yet unknown noise situation in the LAr of the data taking period 1994.

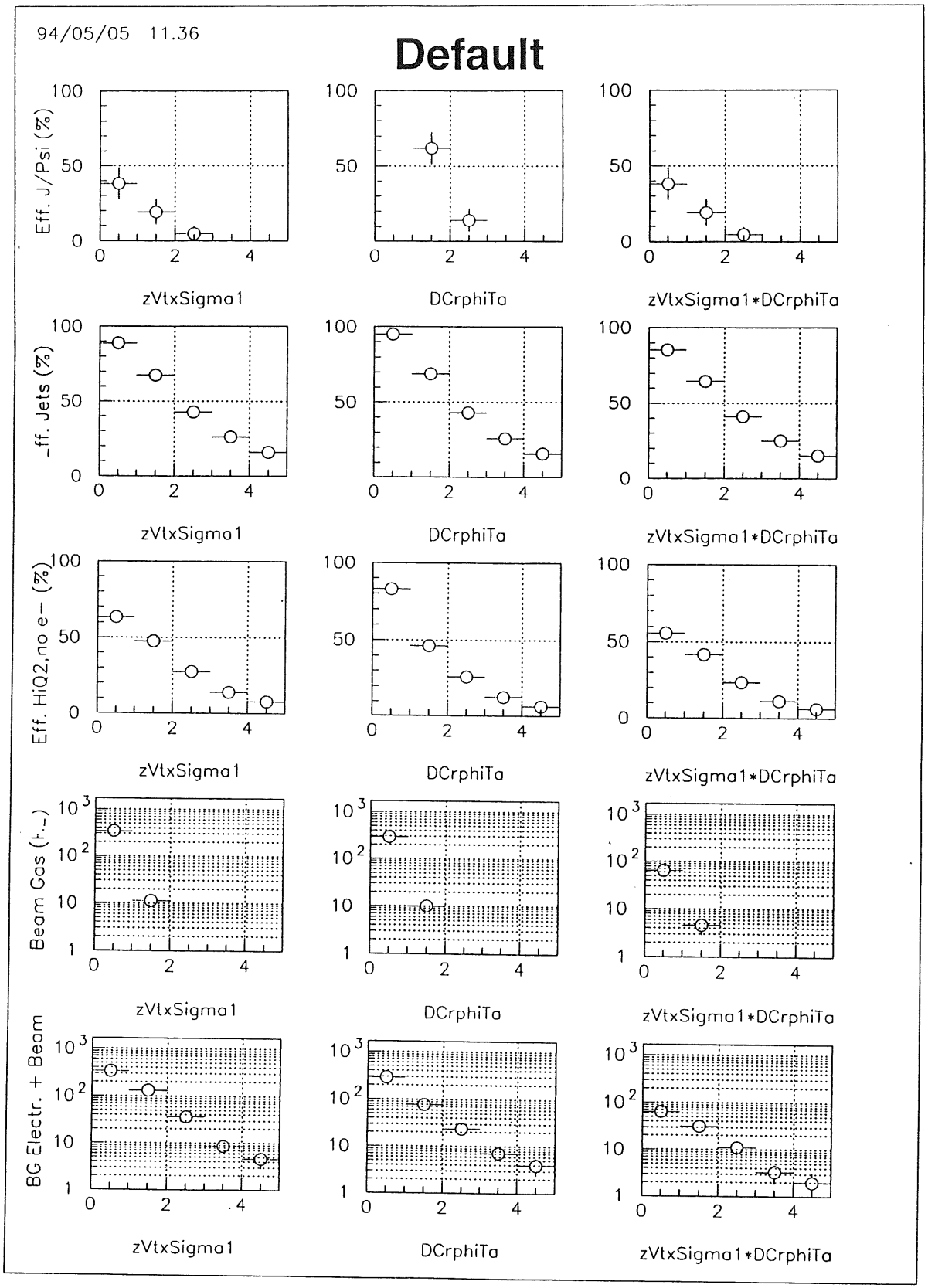

Fig. 5.2. Example of the simulation of one trigger behavior for one setting using the first procedure to simulate the background rates. The x-axis corresponds to the number of validated big towers required.

5.2.2. First Method to Simulate Rates due to Noise

A more complex method was necessary to estimate the background rate due to electronic noise. Since some hard- and software influencing the electronic noise of the LAr system has been changed during the shutdown of this winter, it would not have been sensible to use data from 1993 to get these rates. However a first cosmic run took place in April 1994 and it was therefore possible to take certain information from these new data that were taken with the setup of the LAr trigger as it was expected to be during all the data taking periods 1994. While the electronic noise itself is independent of the beam situation, we have to take care of the fact that the total number of validated big towers is naturally correlated to the number of active big rays and therefore to the activity in the MWPCs. A beam dependency of the 'electronic noise' is therefore to be expected for the big ray trigger.

The simulation of this was done in the following way:

- The cosmic run from April 1994 was analyzed. The correlation of the number of validated big towers versus the number of active big rays was studied for different settings of the big ray trigger. For every number of active big rays, we expected to find a binomial distribution of the number of validated big towers corresponding to a certain validation probability, i.e. the probability that the noise of this big tower exceeds the given threshold. (Fig. 5.3.) Out of the ratio 'validated big towers per active big ray' we calculated the probability that the noise of a big tower exceeded the given threshold.

- Neglecting possible geometrical effects (e.g. that some big towers have a specially high noise rate, that there might be a dependency of the noise rate in θ etc.), this validation probability was assumed to be constant for all the big towers.

- It was then necessary to calculate a new number of validated big towers for every event of the 1993 background sample including this big tower noise validated randomly by big rays. This could only be done by use of a Monte Carlo method. A binomial distribution according to the number of active big rays of the event and the validation probability calculated before were used.

- The result was 'translated' to background-rates.

The shown error bars include only statistical errors due to the final binomial distribution. The error on the value of the validation probability and other systematical effects were not investigated.

Note that this simulation is based only on the number of active big rays per event and does not take in account the geometrical distributions of these big rays. This was first expected to be accurate enough. Later it turned out to be necessary to set up a second method taking in account the different behavior of different big towers.

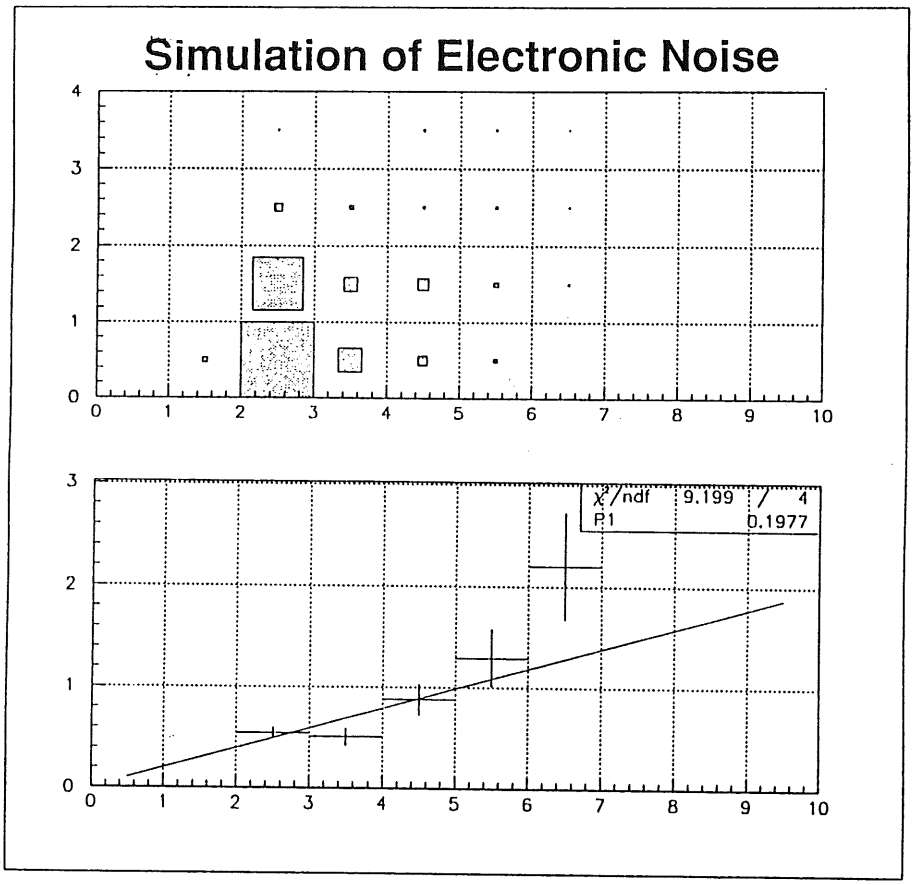

Fig. 5.3. First simulation method based on 1994 cosmic data. The plot shows the number of validated big towers (i.e. big towers with an active big ray and energy above the threshold) versus the number of active big rays. The 'validate ϕ–neighbors' function was on and therefore there are sometimes more validated big towers than active big rays. For every number of active big rays, the mean number of validated big towers was calculated (third plot) and the constant ratio ('P1') was approximated by a fit routine.

5.2.3. Second Method to Simulate Rates due to Noise

Fig. 5.4.1 and 5.4.2. show how often the noise of each big tower exceeded the given thresholds in the 1994 cosmic data; the differences between different big towers are obvious. Fig. 5.5. gives the distribution of active big rays i. e. how often each of them has been switched on for the different classes of events used in the investigations. The plots show that the big rays of the cosmic sample used to determine the validation probability (see chap. 5.2.2) hit mainly very noisy big towers and this probability does therefore not correspond to the average of the detector. Some of the physics (High Q^2) and the background samples are boosted in the forward direction and so they switch on big rays that point to the 'good' regions of the LAr. The first estimation lead therefore to too many enabled noisy big towers and in consequence to a noise rate that is higher than the rate estimated with the second simulation procedure, which pays attention to the specific behavior of different big towers.

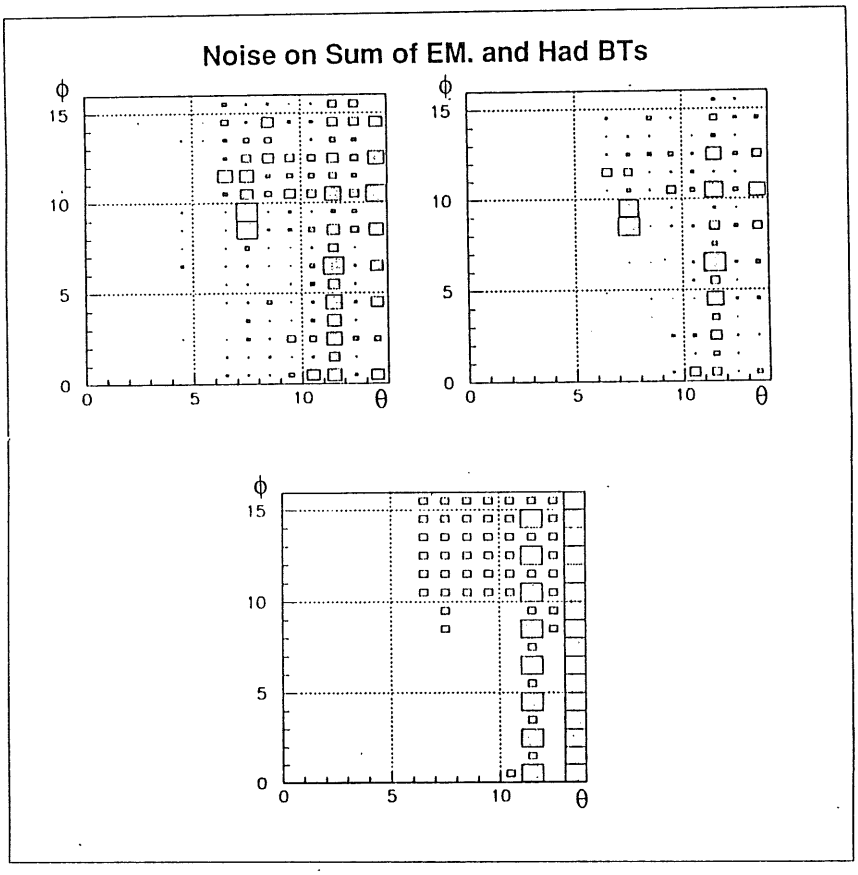

Fig. 5.4. The first two plots show the probabilitiy that electronic noise exceeds the given threshold of 4 and 14 counts (≈125MeV/count) respectively for every big tower. The differences are immense. The third plot shows the three classes we defined (empty=good, small boxes=medium, large boxes=very noisy).

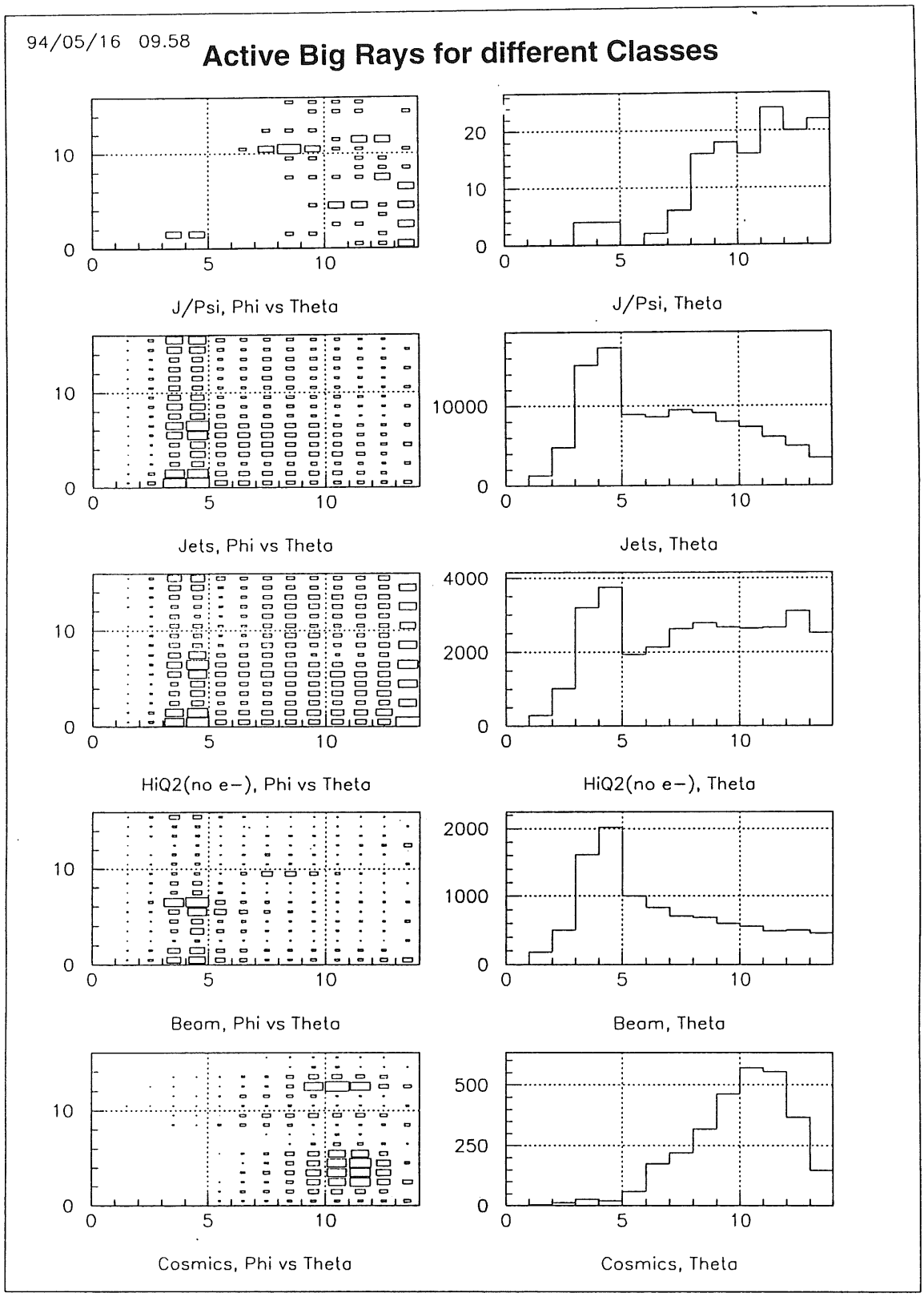

Fig. 5.5. Topologies of different classes of events. The peak at θ = 3 / 4 is due to the 32 - fold segmentation in ϕ.

In the hardware, there is a possibility to set the energy threshold for every big tower independently and to use higher thresholds for the noisy big towers than for the better ones. This lead to the idea to distinguish three groups of big towers: 'very noisy', 'noisy' and 'good'. Fig. 5.4.3. shows these different regions. For each of them, thresholds were simulated independently. Fig. 5.6. shows the probabilities, that the noise of a representative of one of these groups exceeds a given threshold. This plot is again based on the 1994 cosmic run. According to these probabilities and the given thresholds, active big rays pointing to such a big tower were then enabled randomly for the 1993 physics data.

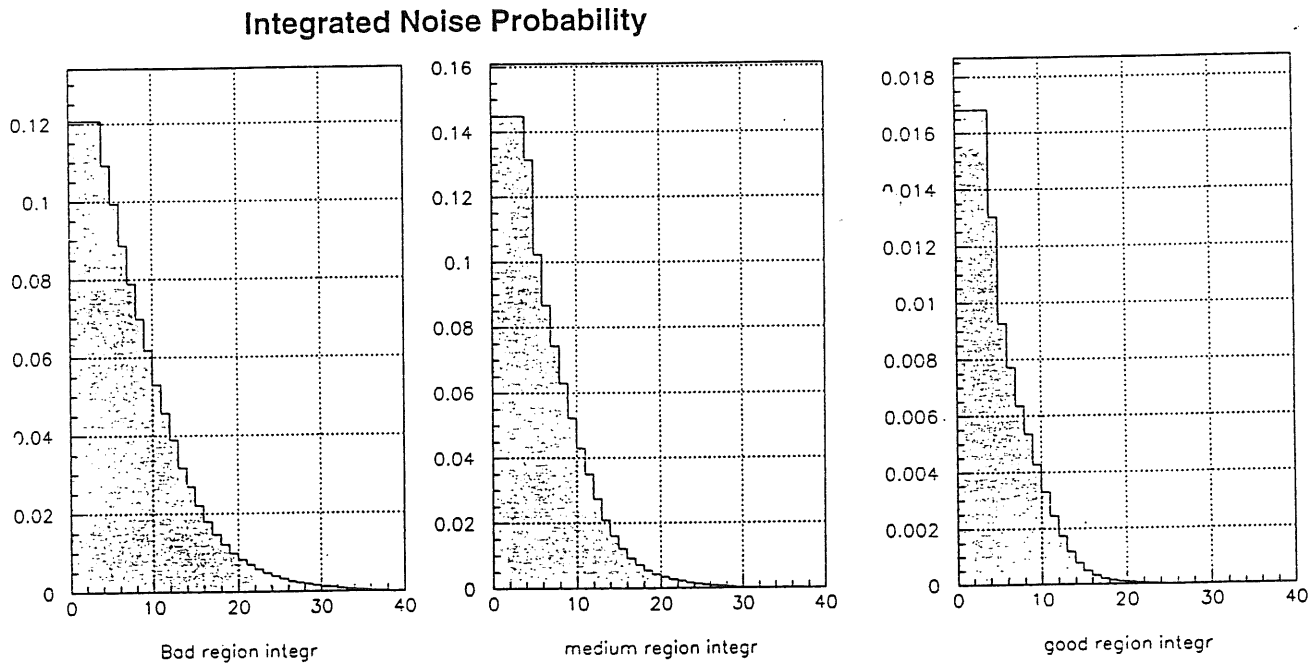

Fig. 5.6. Probability that the noise of a big tower exceeds the given threshold [trigger counts = 125 MeV].

It is to be remarked, that no binomial distribution is needed here any more, as this procedure is executed once for every active big ray whereas the former simulation was based on the total number of active big rays per event. The new procedure did not distinguish between beam-related and electronic noise any more.

We decided to choose the thresholds for the different groups such that the probability to exceed them was the same for every group, lets say 1 or 3 percent. This lead to different thresholds for each group but a noise situation that should be

more or less uniform over all the LAr system. It turned out that for relatively low thresholds there was nearly no difference between 'noisy' and 'very noisy' any more. This means that the definition of the 'very noisy' class was based mainly on rare signals that exceed a very high threshold and not on noise that exceeds an intermediate threshold very often.

5.2.4. Third Method to Simulate Rates due to Noise

End of May 1994 the big ray trigger could be tested for the first time under beam conditions. The thresholds on the energy of the LAr big towers were set to zero which led to very high rates. It was in the following possible to calculate the rates that would have been reached with higher thresholds just by applying the according cuts on the data. No efforts to simulate the noise had to be made any more, as all these effects were now present in reality.

Further analysis of this run showed an important difference between big towers of the forward region and those of the barrel. In Fig. 5.7. the average big tower energy shows a strong dependency in θ. In the first plot, a profile of the number of counts (1 count corresponds to about 125 MeV) in the trigger electronics is given. The second plot shows the same profile for the real energy deposited in the big towers. The rise towards very low values of θ can be seen in both plots and corresponds to real energy deposited mostly by beam-gas events. In the region of the barrel ($\theta > 6$) a difference between the two variables is obvious - the trigger counts in this region are often caused by noise. In a first reaction we defined again two regions: 'forward' ($\theta < 5$) with high thresholds and 'central' where lower thresholds could be set. The positive effect of this classification on the trigger rates can be seen in Fig. 5.8. While the efficiency to detect J/Psi events is not sensitive to the thresholds in the forward direction, Jets and Charged Current events suffer significantly from the very high thresholds at low θ. The background however can be reduced significantly by applying higher thresholds in the forward direction. In a second step, a more sophisticated threshold-distribution for different values of θ was defined which was proposed because smooth functions can better be simulated by the Monte Carlo programs used to determine the efficiencies of the triggers. The values of this threshold-function can be seen in tab. 5.6.

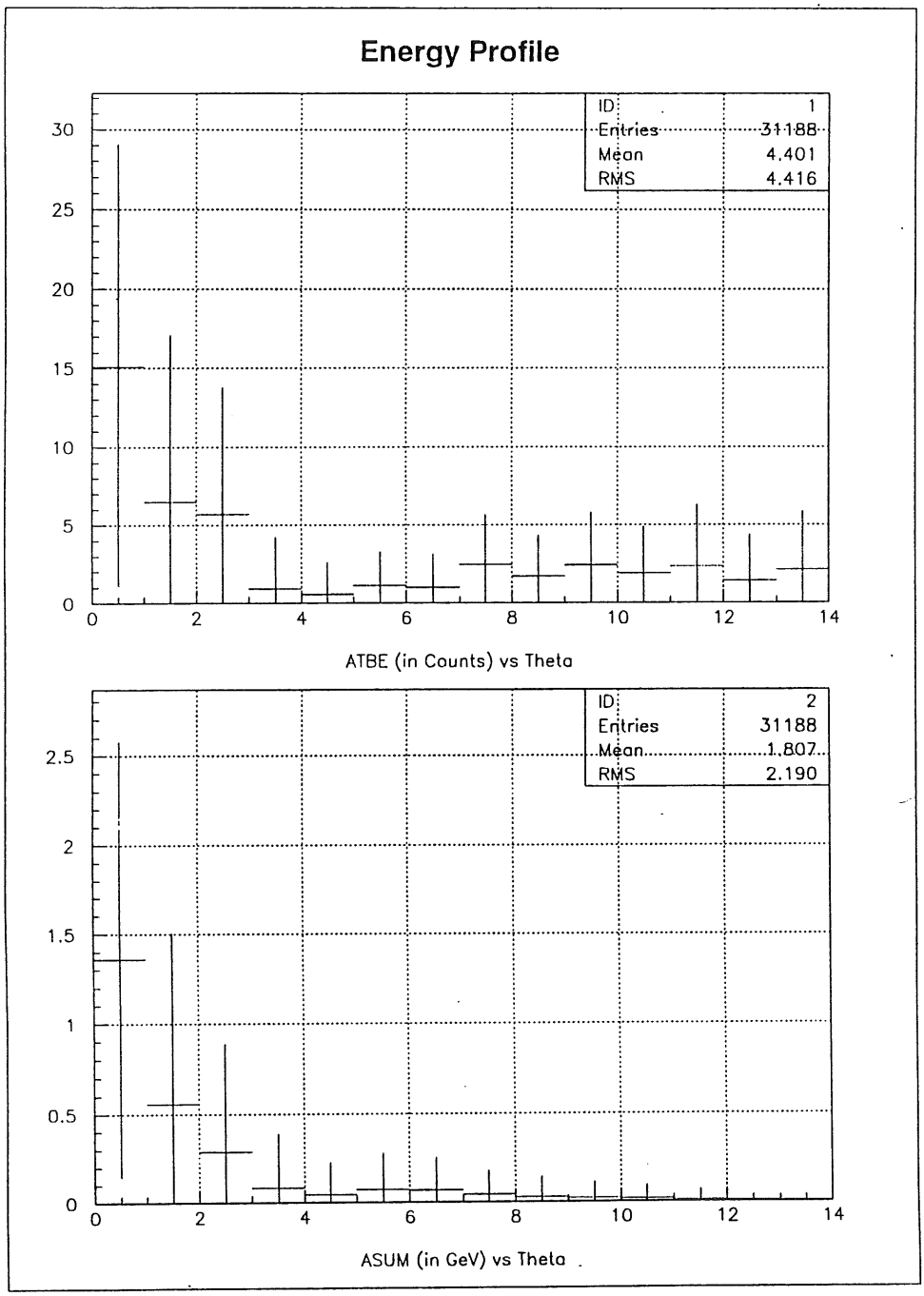

Fig. 5.7. The first plot shows the mean values of background measured by the trigger electronics (1 count ≈125MeV). The second plot shows the real energy. The rise in forward direction corresponds to real energy whereas the trigger energy in the barrel is mainly caused by electronic noise.

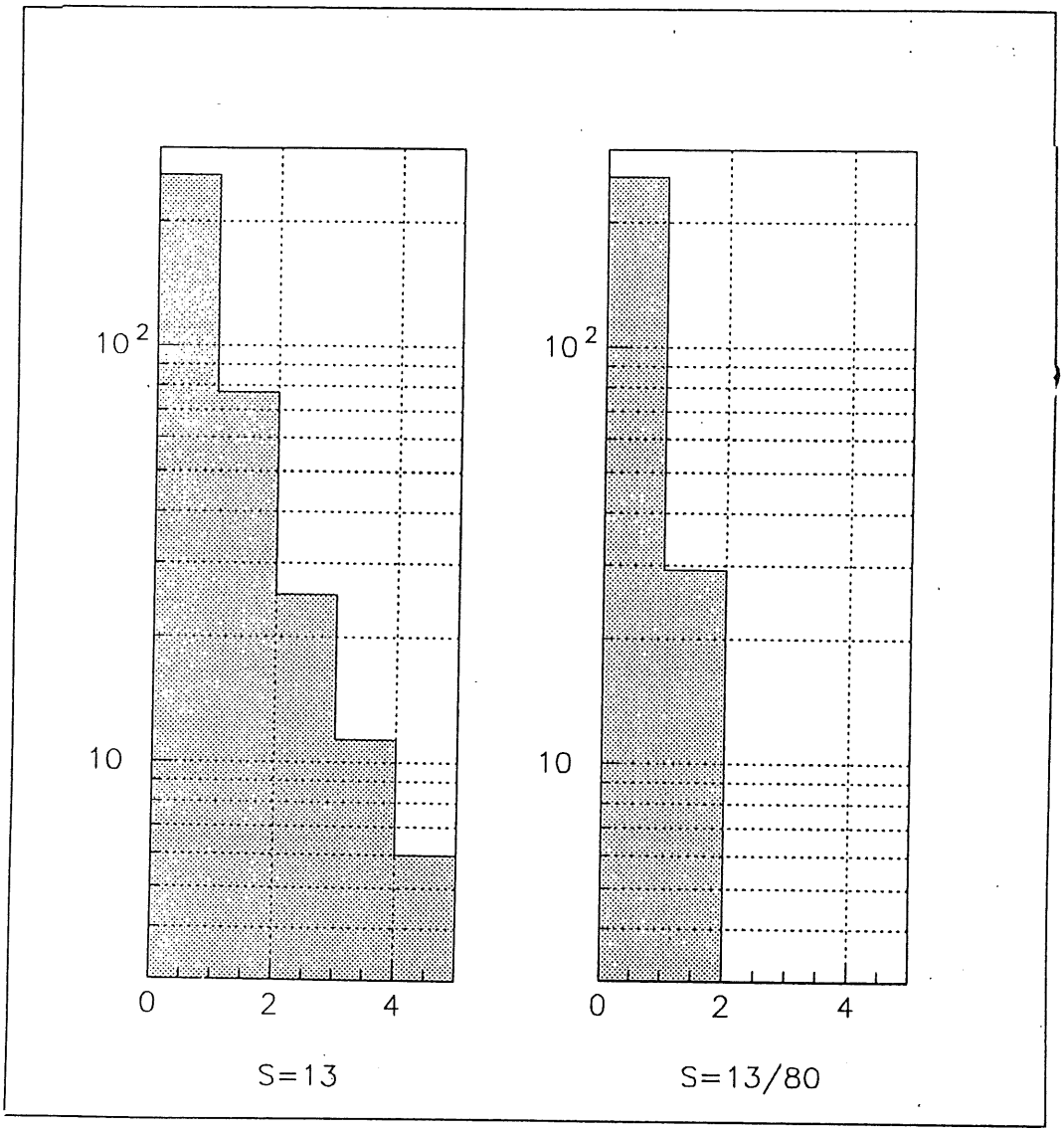

Fig. 5.8. Rates of the LAr big ray trigger if different numbers of validated big towers (0 - 4) are required in coincidence with the z-vertex-sigma1 and the DCrϕTa. A constant energy threshold of 13 counts is compared to a threshold profile with very high thresholds (80 counts = 10 GeV) in the forward direction.

5.2.5. Results

As there are several independent parameters that influence the efficiencies and thus the rates of the big ray trigger, we were forced to concentrate our investigations on a few settings out of all the possible ones. A 'default' was defined, using values that were choosen, as they seemed to be quite reasonable ones just

in the middle of their ranges. These values and their meaning can be seen in tab. 5.1. In the next step one parameter after the other was changed whereby the others always remained at their initial value. In this way we got something like the derivation of the trigger rates and efficiencies to all these parameters.

Name of Variable	**in File**	**Value**	**Meaning**
Version number	CTRC, CTRF	940403	Overlap = 50%
BigRayVal	CTVB	2	Peak +/- 1 selected
N	runa... (anatrig steering file)	disabled	ϕ Neighbors off
S	runa...	7 [125 MeV]	energy threshold to validate big tower

Tab. 5.1. Definition of the 'default' setting.

Variation	**Changed Variable**	**Value**	**Meaning**
Neighbors ON	N	enabled	ϕ Neighbors on
Threshold S=10	S	10 [125 MeV]	higher energy threshold
100% Overlap	Version CTRF CTRC	940405	Overlap = 100%
Peak +/- 2	BigRayVal	3	Peak +/- 2 selected
All Bins selected	BigRayVal	0	All Bins selected

Tab. 5.2. Variations done with the first background simulation procedure.

Variation	Changed Variable	Value	Meaning
S = 19, 16, 5	S (for different Regions)	19 (very noisy), 16 (noisy), 5 (good) always in [125 MeV]	Probability to exceed the threshold is less than 1% for every region
S = 12, 12, 4	S	12, 12, 4 [125 MeV]	Probability is less than 3%
S = 7, 7, 4	S	7, 7, 4 [125 MeV]	Probability is less than 8%

Tab. 5.3. Variations done with the second background simulation procedure.

Variation	Changed Variable	Value	Meaning
S = 40, 11	S (for different Regions)	40 (forward), 11 (barrel), in [125 MeV]	Relatively high rates but good efficiencies expected
S = 80, 13	S	80 (forward) 11 (barrel) in [125 MeV]	Rates not critical but efficiencies rather poor
S = constant	S constant for all θ segments	9, 13, 17 ea..	Rates are clearly dominated by the big towers in forward direction

Tab. 5.4. Variations done with the third background simulation procedure.

1st simulation Procedure	Efficiency [%] J/Psi s50	s52	Efficiency [%] Jets s50	s52	Efficiency [%] Hi Q^2 s50	s52	Background Rate [normalized] s50	s52
Default	05	55	40	00	25	05	**1**	**1**
ϕ-Neighbors ON	10	60	55	00	30	05	2.5	1.8
S = 10	05	45	25	00	20	00	0.28	0.50
100% Overlap	05	55	45	00	30	05	1.4	1.1
Peak +/- 2	05	55	45	00	30	05	1.5	1.1
All Bins selected	05	55	55	00	30	05	2.5	1.5
3rd simulation Procedure	**Efficiency [%] J/Psi s50**	**s52**	**Efficiency [%] Jets s50**	**s52**	**Efficiency [%] Hi Q^2 s50**	**s52**	**Background Rate [normalized] s50**	**s52**
S = 13 / 13 (constant)	05	35	35	00	20	05	**1**	**1**
S = 11 / 40 (central / forward)	00	45	45	00	30	05	0.9	1.6
S = 13 / 80	00	35	25	00	20	00	0	0.50

Tab. 5.5. Efficiencies and rates simulated for the new subtriggers (see page 56). The simulated rates differ between the three simulation procedures. Therefore they are normalized for each simulation procedure to the first setting listed here.

5.2.6 Conclusions

The simulations allowed to get a first impression of the behavior of the new trigger and we were then to choose the settings for the data taking period 1994 on base of these predictions. Tab. 5.5. shows the effects of the different variables. The following observations were made:

- Subtriggers: It is obvious that the big ray trigger has to be combined with other L1 systems. The DCrϕ trigger and the used z-vertex Quality bits proved to be quite good for this purpose. Therefore the following new subtriggers were created:

  s 50: DCrϕTa * zVtx_sigma1 * (LAr_BR > 1)*

  s 52: DCrϕTa * zVtx_small * (LAr_BR > 0)*

- 'ϕ Neighbors ON' increases the efficiency about 5% for the charged current events and 5-10% for the jets. The background rate however is quite sensitive to this parameter and it seems therefore to be recommended to use this option only for the θ segments with eight fold ϕ segmentation.

- The difference between 50% and 100% overlap in θ (see chap. 3.1.) is very small - an increase in the efficiency can be seen for the jets whereas nothing can be said about the background rates as the difference seems to be at level of the statistical uncertainties due to the Monte Carlo simulation method. It therefore seems to be advisable to use the netlist based on a 100% overlap as this one has already been used for the test runs.

- The 'Bin Selection' method has relatively little influence on the efficiencies for the different classes of physics events (only apparent at the jets sample) - the noise rate however can be reduced by a significant factor, if not all bins are selected. The difference between 'Peak +/-1' and 'Peak +/-2' however is very small. Only for the 'jets' sample, an increase of 3-5% of the efficiency can be observed when the bins next but one to the peak are selected as well. The noise rate is about the same. I would propose therefore to use 'Peak +/-2' as this Xilinx program has already been used for all the test runs and we are therefore relatively sure that there are no errors in this Xilinx configuration.

* (LAr_BR>n) means, that more than n validated big towers with an energy above the given threshold are required.

- Quite a lot of different settings of the thresholds have been tested. It is obvious that the trigger becomes more selective when different thresholds are used for different classes of big towers. The behavior of the LAr that caused our first classification of big towers in April 1994 did not appear in the data of May any more. The θ-dependent thresholds as discussed in 5.2.4. however seem to be quite useful.

Tab. 5.6. Threshold profile

θ	0 - 3	4	5	6 - 13
Threshold [125 MeV]	80	40	20	14

In the first luminosity runs of 1994 with the new trigger, the following rates were measured:

s 50:	≈ 1.5 Hz
s 52:	≈ 5.0 Hz
Proton current:	≈ 40 mA
Electron current	≈ 15 mA

The definitive settings were:

φ - Neighbors:	OFF
Overlap:	100%
Bin Selection Method:	Peak +/- 2
Energy - Threshold S:	as shown in Tab. 5.6.

Page 59:

Fig. 5.9. Example of an event triggered by the new subtrigger 50 in summer 1994. This event and the following one were taken out of a sample of J/Psi candidates. The plots on the right side show the energies in MeV.

Page 60:

Fig. 5.10. A J/Psi candidate triggered by the new subtrigger 52 in summer 1994. The real energy of the validated big tower is slightly below the required threshold of 1750 MeV. It was nevertheless validated thanks to the uncertainties of the energy measurement in the trigger electronics.

94/08/05 14.36

Run 76491 Evt 704, Subtr 50

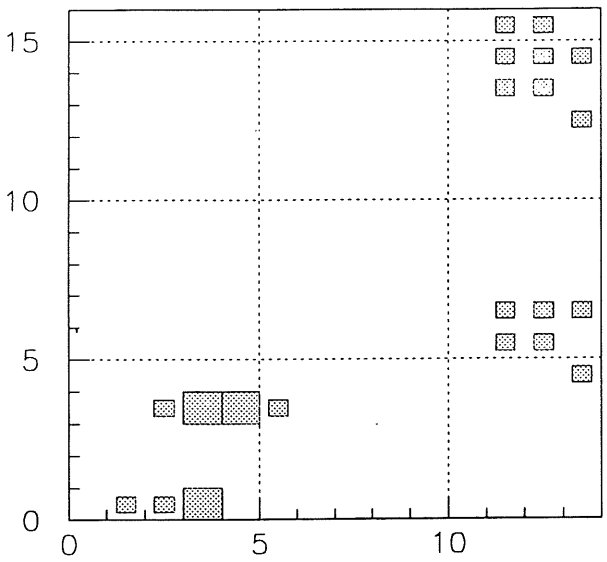

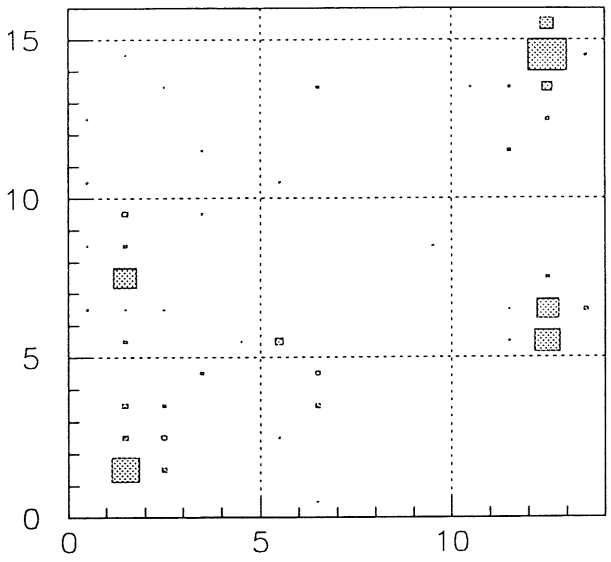

active big rays

total BT energy

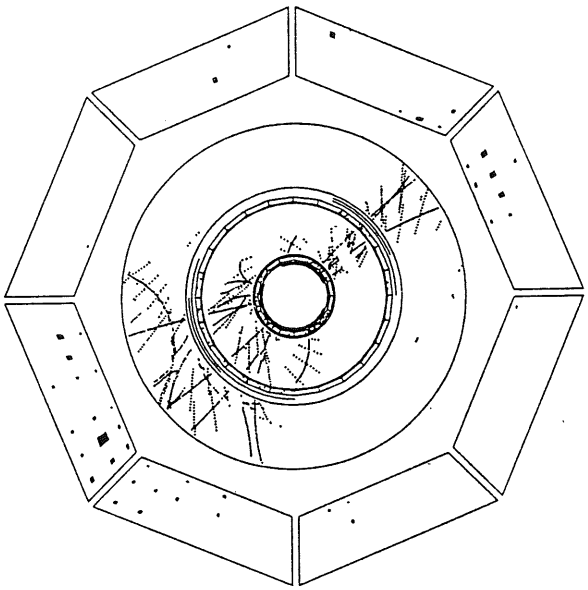

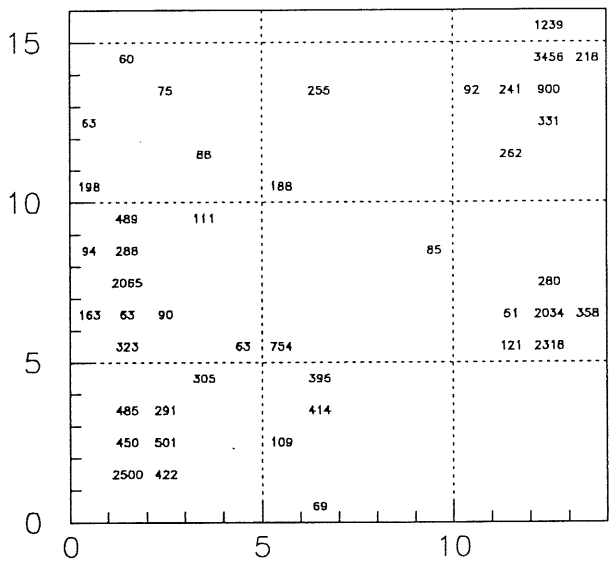

Y
X

total BT energy

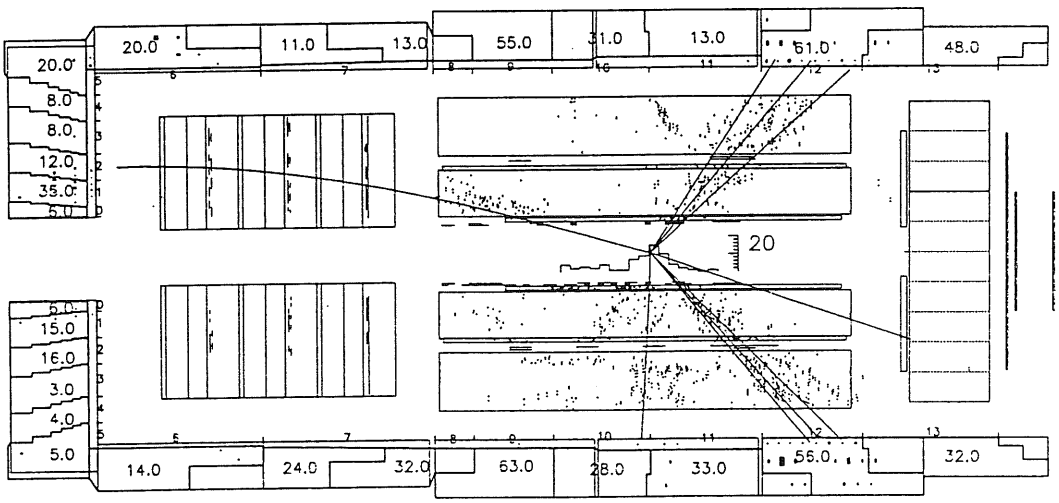

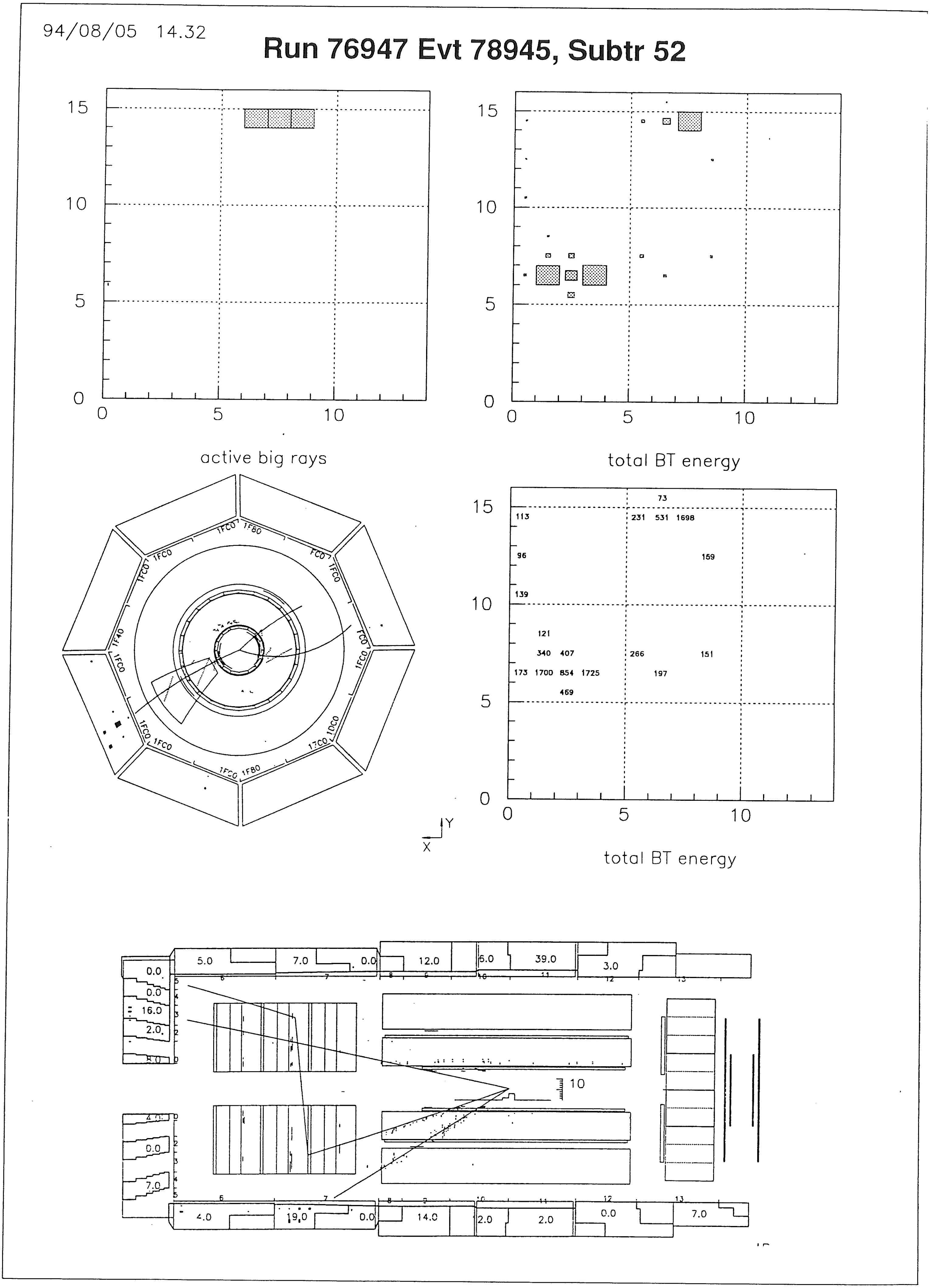
94/08/05 14.32
Run 76947 Evt 78945, Subtr 52
active big rays
total BT energy
73
113
231 531 1698
96
159
139
121
340 407
266
151
173 1700 854 1725
197
469
total BT energy
Y
X
5.0
7.0
0.0
12.0
6.0
39.0
3.0
16.0
2.0
10
4.0
19.0
14.0
2.0
7.0

Bibliography

[1] S.Eichenberger, Development of the Ray Finder Electronics for the z-Vertex Trigger for the H1 Detector at HERA, Diploma Thesis, University of Zurich (1988), H1 collaboration internal report H1-11/88-96

[2] S.Eichenberger, A Fast Pipelined Trigger for the H1 Experiment at HERA Based on Multiwire Proportional Chamber Signals, Ph. D. Thesis, University of Zurich (1993)

[3] G. Wolf, HERA Physics (1994), DESY report 94-022

[4] H1 Collaboration: I. Abt et al., The H1 detector at HERA, DESY report 9/93-103

[5] XILINX: The Programmable Gate Array Data Book, XILINX Inc., 2100 Logic Drive, San Jose, CA 95124, USA

[6] MacIntosh Programmers Workshop, Apple Computer, Inc., 20525 Mariani Avenue, Cupertino, CA 95014, USA

[7] Inside MacIntosh I-V, Apple Computer, Inc., 20525 Mariani Avenue, Cupertino, CA 95014, USA

Acknowledgements

During this work, I could make a lot of good and interesting experiences.
I am really thankful for the opportunity I was given to solve theoretical and technical problems with such a large degree of freedom and to get this insight into the fascinating experiment H1.

'Thank You' to all the people who helped and motivated me during this time, especially Ueli Straumann, the whole group of Prof P. Truöl at the H1 Experiment and many others.